Helsinki University of Technology
Department of Electrical and Communications Engineering
Laboratory of Electronics Production Technology
Espoo 2001

TANTALUM-BASED DIFFUSION BARRIERS FOR COPPER METALLIZATION

Tomi Laurila

Dissertation for the degree of Doctor of Science in Technology to be presented with due permission of the Department of Electrical and Communications Engineering, Helsinki University of Technology for public examination and debate in Auditorium S5 at Helsinki University of Technology (Espoo, Finland) on the 14th of December, 2001, at 12.

ABSTRACT

Interfacial reactions between Cu and Si with different Ta-based diffusion barriers are investigated by means of the combined thermodynamic-kinetic and microstructural analysis. The reaction mechanisms and the related microstructures in the Si/Ta/Cu, Si/TaC/Cu and Si/Ta_2N/Cu metallization systems are studied experimentally and theoretically by utilizing the ternary Si-Ta-Cu, Si-Ta-C, Si-Ta-N, Ta-C-Cu, and Ta-N-Cu phase diagrams as well as the activity diagrams calculated at different temperatures. The effects of oxygen on the reactions in the Si/Ta/Cu and Si/TaC/Cu metallization systems are investigated by employing also the evaluated Ta-O and Ta-C-O phase diagrams. The experimental investigations are carried out with the help of sheet resistance measurements, x-ray diffraction (XRD), Rutherford backscattering spectroscopy (RBS), scanning electron microscopy (SEM), secondary ion mass spectroscopy (SIMS) and transmission electron microscopy (TEM). It is shown that by using the combined thermodynamic-kinetic approach a better understanding about the reactions taking place in the Si/Cu diffusion couples with different Ta-based diffusion barriers can be achieved. The diffusion barrier solutions using Ta are good candidates for practical applications.

PREFACE

The work for this thesis has been carried out at the Department of Electrical and Communications Engineering of the Helsinki University of Technology between June 1998 and June 2001. I am very grateful to my supervisor Professor Jorma Kivilahti for his guidance, support and time. His continuous remarks and counseling regarding the theoretical as well as practical aspects of this thesis provided important and essential knowledge which helped in completing the work. His enthusiasm to understand different materials in detail as precisely as possible has been a constant source of inspiration.

I am also indebted to the following people at the VTT Microelectronics in Otaniemi: Jyrki Molarius whose expertise in thin film deposition and experience from the field of diffusion barriers provided strong support for this thesis. Ilkka Suni with his continuous reminding of the practical constraints and the applicability of this investigation contributed greatly to this work. I would also like to acknowledge Tommi Riekkinen for preparing some of the diffusion barrier layers.

I want to thank all the people in the Laboratory of Electronics Production Technology. Especially I would like to mention Kejun Zeng and Vesa Vuorinen for the very useful discussions and Pia Holmberg for her assistance in the world of bureaucracy, which was and still is so strange to me. Markus Turunen and Toni Mattila have also contributed to this thesis not only as colleagues but also as friends.

I want to dedicate this thesis to the memory of my father and greatly thank my mother and brother for their love and support.

Finally I want to thank my wife Marjut for her endless love and support during the years. There exist no words glowing enough to describe my gratitude to her.

Espoo, June 2001
Tomi Laurila

NOTATION

a_i	activity of component *i*
A_{gb}	cross-section of grain boundaries per unit area
A_l	cross-sections of grains per unit area
c_i	concentration of component *i*
c	number of components
C	capacitance
d	average grain diameter
$\tilde{D}$	interdiffusion coefficient
D_i	intrinsic diffusion coefficient of component *i*
D_i^*	tracer diffusion coefficient of component *i*
D_o	pre-exponential factor
D_{gb}	grain boundary diffusion coefficient
D_{tot}	total effective diffusion coefficient
D_{vol}	volume diffusion coefficient
D_{T_m}	self-diffusion coefficient at the melting point
f	degrees of freedom
G	Gibbs free energy
DG_m	Gibbs free energy of mixing
D_rG	Gibbs free energy of reaction
D_rG^o	standard Gibbs free energy of reaction
H	entalphy
DH_m	entalphy of mixing
J_i	flux of component *i*
K_p	equilibrium constant
l	distance
L_i	phenomenological coefficient of component *i*
$M(t)$	number of atoms transported per unit area and unit time
n_i	number of moles of component *i*

p	pressure or number of phases
Q	activation energy
R	gas constant or resistance
S	entropy
DS_m	entropy of mixing
t	time
T	temperature (K)
T_m	melting point
U	internal energy
$v^{K/M}$	velocity of the Kirkendall-plane respect to the Matano-plane
V	volume
V_i	partial molar volume of component i
V_m	molar volume
x_i	mole fraction of component i
d	conventional thickness for grain boundaries
g_i	activity coefficient of component i
m_i	chemical potential of component i
m_i^o	chemical potential of component i in its standard state

List of Publications

Appendix I — T. Laurila, K. Zeng, J. Molarius, I. Suni, and J.K. Kivilahti, "Chemical Stability of Tantalum Diffusion Barrier Between Cu and Si", *Thin Solid Films*, **373**, (2000), pp.64-67.

Appendix II — T. Laurila, K. Zeng, J. Molarius, I. Suni, and J.K. Kivilahti, "Failure Mechanism of Ta Diffusion Barrier Between Cu and Si", *Journal of Applied Physics*, **88**, (2000), pp.3377-3384.

Appendix III — T. Laurila, K. Zeng, J. Molarius, I. Suni, and J.K. Kivilahti,"Effect of Oxygen on the Reactions in the Si/Ta/Cu Metallization System", *Journal of Materials Research*, **16**, (2001), pp.2939-2946.

Appendix IV — T. Laurila, K. Zeng, J. Molarius, T. Riekkinen, I. Suni, and J.K. Kivilahti, "Tantalum Carbide and Nitride Diffusion Barriers for Cu Metallisation", *Microelectronics Engineering*, **60**, (2001), pp. 71-80.

Appendix V — T. Laurila, K. Zeng, J. Molarius, I. Suni, and J.K. Kivilahti, "Stability of TaC Diffusion Barrier Between Si and Cu", HUT Internal Report, HUT-EPT-7, ISBN 951-22-5777-7, (2001). This report is composed of two manuscripts: “TaC as a Diffusion Barrier Between Si and Cu" (submitted to *Journal of Applied Physics*) and "Amorphous Layer Formation at the TaC/Cu Interface in the Si/TaC/Cu Metallization System" (submitted to *Applied Physics Letters*).

The research program has been planned by the author together with the co-authors J.K. Kivilahti and J. Molarius. The thermodynamic evaluations needed in this work were carried out jointly by the author and the co-author K. Zeng. The author also participated into all aspects of the experimental and the analytical work executed during the investigations. The theoretical considerations as they appear in the manuscripts were produced by the author in collaboration with the co-authors. The author wrote the manuscripts, which have been discussed in detail with the co-authors.

1. Introduction

The current trend of scaling down the dimensions of integrated circuits in order to achieve better electrical performance places serious demands for materials used in silicon based devices. In particular, thin film interconnections are becoming the limiting factor in determining performance and reliability of integrated circuits. The interconnection delay, usually defined as the *RC*-delay, where *R* is the resistance of the interconnection and *C* is the associated total capacitance, is one of the most important factors determining the device/circuit performance [1]. Reducing the *RC*-delay to lower than or to equal to the device delay has become both a material and an interconnection design/architecture challenge. Aluminum has been the most widely used material for metallization in very-large-scale integration (VLSI) and ultralarge-scale integration (ULSI) circuits during the past decades. However, as critical dimensions of devices have approached submicron dimensions, reliability requirements has ruled out the possibility of using pure aluminum. In order to improve reliability, alloys with several additives such as Si, Cu, Ti, Pd, Cr, Mg and Mn, have been tested [2]. The improvement in the electromigration performance thus achieved remains to date limited and is offset by the corresponding increase in interconnection resistivity [2].

Hence, emphasis and burden have been placed on materials *e.g.*, switching from Al/W based metallisations to Cu based interconnections. Unfortunately, the interaction between Si and Cu is rapid and detrimental to the electrical performance of Si even at temperatures below 473 K [3-6]. Mobility of copper is also relatively fast in SiO_2 and many polymers used as dielectric layers [7,8]. Moreover, copper corrodes easily upon exposure to moisture or oxygen and a technique to passivate the copper surface is essential for multilevel copper interconnection [9]. Therefore, owing to these multiple material problems (see Fig. 1), it is necessary to implement a barrier layer into the Cu metallization scheme and to encapsulate copper conductors from all sides. In this respect, diffusion barriers in Cu metallizations differ from the ones used in Al metallizations, where a diffusion barrier is generally used only at one interface (Fig. 2). The need to

encapsulate Cu conductor imposes also boundary conditions for diffusion barrier thickness.

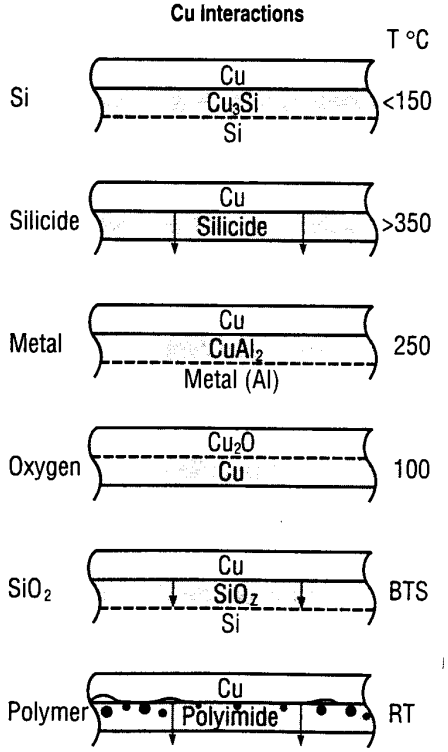

Figure 1. Schematic presentation of the problems related to Cu metallizations [7].

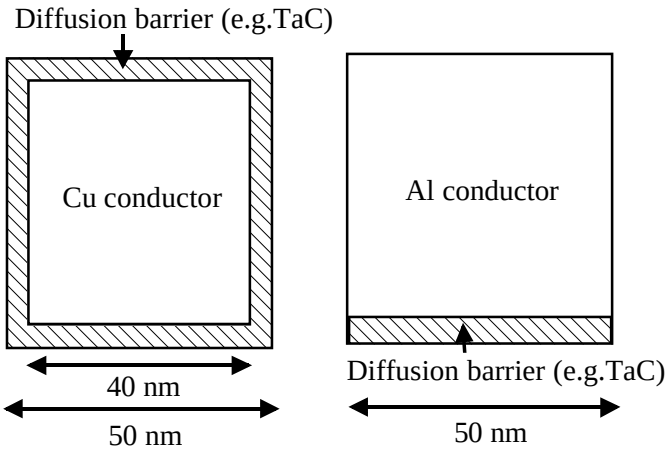

Figure 2. Schematic presentation of the difference in diffusion barrier implementation between Cu and Al conductors.

The diffusion barrier layer reduces the cross-sectional area of Cu conductor and thereby increases the effective resistance of the interconnection. Therefore, in order to have the maximum advantage from switching to Cu interconnections, the barrier layer thickness should be less than 10 nm [10].

In addition to the problems mentioned above there are also processing difficulties related to copper. For example, patterning of Cu by reactive ion etching (RIE) is a difficult task because of high temperatures needed and narrow processing window allowed [11]. Therefore, processes like chemical mechanical polishing (CMP) have to be utilized instead [12-14].

2. Diffusion Barriers in Cu Metallization

The harmful interaction between Si and Cu, as mentioned in the previous chapter, imposes the use of diffusion barriers in order to reliably fabricate copper metallised IC's. The most important barrier properties are considered in this chapter. First the concept of a diffusion barrier is introduced and then thermodynamic and kinetic as well as microstructural properties are reviewed. Finally, several diffusion barrier solutions as found from the literature are summarized.

2.1 The concept of a diffusion barrier

The concept of the use of barrier layers in metallization systems is simple: two materials that have unfavorable chemical interaction are kept separate by an intermediate layer. Such a barrier should posses several features, which include [15,16]:

(1) If the barrier layer X separates materials A and B, the barrier should be thermodynamically stable when in contact with both A and B.
(2) X should prevent harmful interdiffusion between A and B. Thus, diffusivity of both materials A and B in barrier layer should be as low as possible. The most preferred structure would be single-crystalline, but this solution lies generally beyond the

capabilities of current technology. A practical second choice is the amorphous structure (this is, however, in contradiction with the requirement for the thermodynamic stability).

(3) The barrier layer should form low resistance contacts with both materials A and B and be at least a reasonable thermal conductor. The resistivity of the barrier layer itself is usually not too significant up to a certain point (< 2500 μΩcm) [17] because of its small thickness compared to that of the materials A and B.

(4) X should adhere well to all materials used in the metallization scheme. Thus, some reactivity is required in order to establish good adhesion between the barrier and the surrounding materials.

(5) The material X should not have an electrochemical potential very different from that of A and B in order to avoid the formation of galvanic corrosion cells with the metallization layers.

(6) Stresses of around GPa are expected to exert significant effects upon thin-film diffusion processes [18]. Therefore, stresses in the barrier material should not be too high.

As can be seen from the list of requirements, compromises are often needed and some contradictions cannot be avoided. In addition to the physicochemical demands also process conditions related to step coverage, capability of selective patterning, reasonable rate and ease of deposition and so on, must be fulfilled in order to have a satisfactory diffusion barrier.

Practical diffusion barriers are generally divided into (i) sacrificial barriers, (ii) stuffed barriers, and (iii) amorphous diffusion barriers [16]. The idea of sacrificial barrier is that the intermediate layer X reacts either with one or both of the materials A and B in a laterally uniform manner with characterized reaction rates. The effectiveness of the barrier is determined by the reaction rate. As long as the intermediate layer is not completely consumed in the reactions, the separation between the materials A and B is still effective. Therefore, reaction rate between X and A or/and B should not be too high in order to have effective barrier layer. This definite lifetime is also the major limitation

of sacrificial barriers. For a more permanent protection the barrier layer X should be thermodynamically stable against A and B. This means that there are no driving forces for reactions at the interfaces A/X and X/B. This is necessary but not sufficient condition for a stable diffusion barrier. It is also necessary to stop or reduce diffusion of A and B across X via short-circuit paths, since there is still a driving force for A to diffuse into B and *vica versa*. This can be achieved either by (1) eliminating the short-circuit paths or (2) fill the easy paths with appropriate atoms/molecules and thereby prevent the short-circuit diffusion of A and B [16]. The second approach leads to the concept of stuffed barrier. When atoms of A and B cannot use the short-circuit paths (they are now occupied by the atoms or molecules introduced there on purpose) diffusion is slowed down generally by several orders of magnitude. The elimination of short-circuit paths can also be achieved by removing the easy paths (*i.e.* grain boundaries) by making the structure of the barrier amorphous. It is emphasized that amorphous layers are metastable and will eventually crystallize. When crystallization takes place, grain boundaries are again present in the barrier. Thus, crystallization temperature of amorphous layer is of critical importance. The fabrication of amorphous layers and other related issues are further discussed in Ch. 2.4.

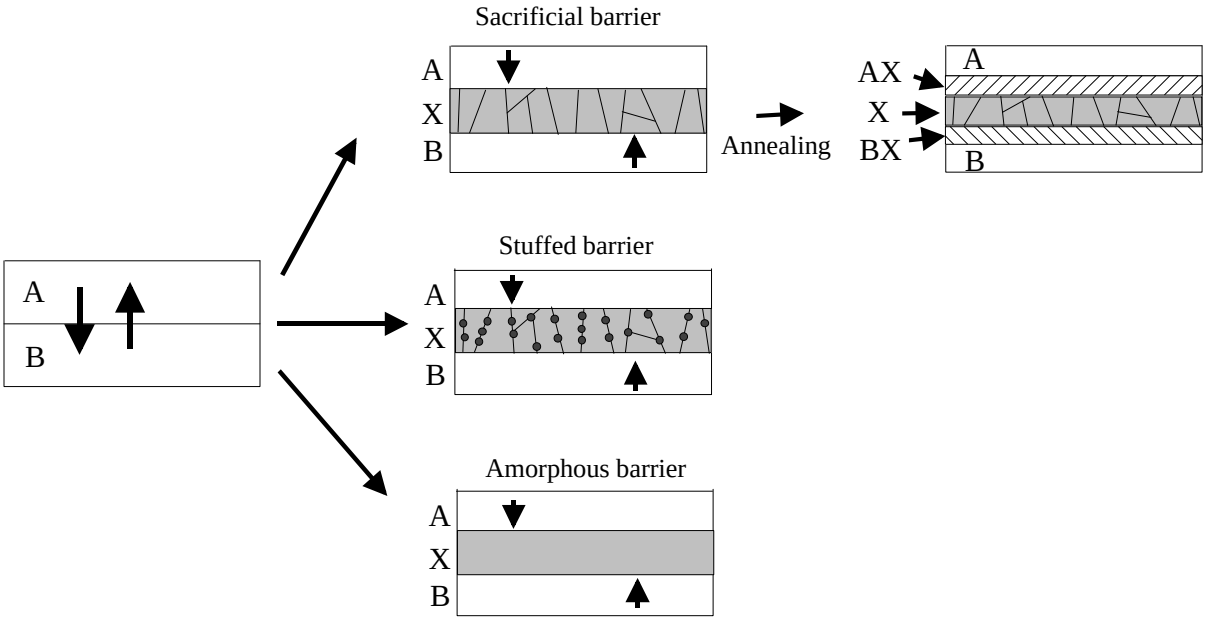

Fig 3. Schematic illustration of the three classes of diffusion barriers.

2.2 Thermodynamic properties

Metallization structures used in microelectronics are composed of many dissimilar materials. In order to be able to predict the feasibility of the interconnection structures, the stability of the interfaces between different materials should be known as thoroughly as possible. When two solids (A and B) are in contact an interphase is formed between them. The total Gibbs free energy of the system (A/interphase/B) can decrease by different processes such as: enrichment of the components in the interphase with respect to one or both of the components or via chemical reaction of components followed by the formation of additional phase(s). When the pressure and the temperature of the system are constant and the interfaces between different phases are macroscopically planar, the change in the Gibbs free energy of the system can be used as criteria for possible reaction products that can form at the interface. In the thermodynamic treatment of multicomponent mixtures or solutions the activities of each component are needed (Ch. 2.2.2). The phase rule, which provides the basis for the presentation of phase equilibria, like the equilibrium phase diagrams, is also important when determining the degrees of freedom of the equilibrium system. These thermodynamic properties are introduced and discussed in the following section.

2.2.1 Gibbs free energy and thermodynamic equilibrium

The function by means of which the combined statement of the first and second laws of thermodynamics can be stated in terms of temperature (T) and pressure (p) is the Gibbs free energy. The Gibbs free energy of a closed system is defined by the relation:

$$G \equiv U + pV - TS = H - TS\,, \qquad (1)$$

where U, V, H, and S are the internal energy, the volume, the enthalpy and the entropy of the system, respectively. Given that $G = G(T,P,n_1, n_2,...)$ in an open system, with n_i being the number of moles of component i, the derivative of Eq. (1) yields:

$$dG = -SdT + Vdp + \sum_i \mu_i dn_i \qquad (2)$$

where μ_i is the chemical potential of component i. At a constant value of the independent variables P, T and n_j $(j \neq i)$ the chemical potential equals the partial molar Gibbs free energy, $(\partial G/\partial n_i)_{P,T,j \neq i}$. With the help of the Gibbs free energy function the equilibrium state of the system can be investigated.

Three stable equilibrium states to be considered are (i) complete thermodynamic equilibrium, (ii) local thermodynamic equilibrium and (iii) partial thermodynamic equilibrium. When the system is at complete equilibrium its Gibbs free energy (G) function has reached its minimum value, $dG = 0$ *or* $\mu_i^a = \mu_i^b = ... = \mu_i^f = 0$, ($i$ = *A,B,C,...*) and then the system is in mechanical, thermal and chemical equilibrium with its surroundings. Thus, there are no gradients inside the individual phases.

On the other hand, local equilibrium is defined in such a way that the equilibrium exists only at the interfaces between different phases present in the system. This implies that the thermodynamic functions are continuous across the interface and the compositions right at the interface are very close to those indicated by the equilibrium phase diagram. Since the complete thermodynamic equilibrium is seldom achieved in thin film systems, the concept of the local equilibrium is central for this thesis. The local equilibrium is generally treated with the help of the chemical potential, which is further discussed in Ch. 2.2.2.

Partial equilibrium means that the system is in equilibrium only with respect to certain components. It is generally found that some processes taking place in the system can be rapid while others are relatively slow. If the rapid ones occur fast enough to fulfil the requirements for complete equilibrium (within the limit of error) and the slow ones slow enough that they can be ignored, then it is quite proper to treat the system as being in equilibrium with respect to the rapid processes alone [19].

As the classical thermodynamics does not include time as a variable, the lowest possible energy state of the system (*e.g.* global minimum) may not be reached in reasonable time, and some other local minimum is attained. In such case one is dealing with metastable equilibrium. In fact, a principle commonly known as *Ostwald's rule* states that, when a system undergoing reaction proceeds from a less stable state, the most stable state is not formed directly but rather the next more stable state is formed, and so on, step by step until (if ever) the most stable is formed [19]. It is a fact that most materials used in everyday life have not been able to reach their absolute minimum energy state and are therefore in metastable equilibrium. It should be noted that a system at metastable equilibrium has as exactly determined thermodynamic properties as a system at stable equilibrium.

Finally, it must be emphasized that when the Gibbs free energy function corresponding to the equilibrium state (either stable or metastable) of the system is defined, all other equilibrium properties of the system are also fixed. This enables the extrapolation of great amount of thermodynamic data, such as activities of the components, chemical potentials of the components, heat capacities, enthalpy, entropy and so on, from the Gibbs free energy function. These data in turn provides lots of information that can be used to describe the system thermodynamically in the form of phase diagrams, stability diagrams, *etc.*, as will be seen later on.

2.2.2 The chemical potential and activity in a binary solid solution

It is common knowledge that most substances in nature consist of several phases, and that the phases are seldom pure substances. In fact, a pure substance exists only in our minds and represents a limiting state, which we may asymptotically approach but never actually obtain. Thus, the thermodynamic description of multicomponent systems is of great importance from the theoretical as well as from the practical point of view. In the treatment of multicomponent open systems, the most common process considered in defining the thermodynamic functions for a solution is called the mixing process. The mixing process is the change in state experienced by the system when appropriate

amounts of the "pure" components in their reference states are mixed together forming a homogeneous solution brought to the same temperature and pressure as the initial state [20]. The molar Gibbs free energy of mixing, or the molar Gibbs free energy of formation of solution, can be expressed as follows:

$$\Delta G_m = \Delta H_m - T\Delta S_m \qquad (3)$$

It is to be noted that although mixing process is strongly influenced by interaction forces between atoms and molecules (*i.e.* DH_m) , the fundamental cause behind mixing is entropy (DS_m).

For any heterogeneous system at equilibrium, the chemical potential of a component *i* has the same value in all phases of the system. An example of a binary phase diagram with limited mutual solubility of the components is presented in Fig. 4 (a). Between the homogeneous terminal phases α and β there is a two phase region, where α and β coexist. The corresponding Gibbs free energy diagram is shown in Fig. 4 (b). It should be noted that both phases α and β have their individual molar Gibbs free energy curves and thus the components have different crystal structures.

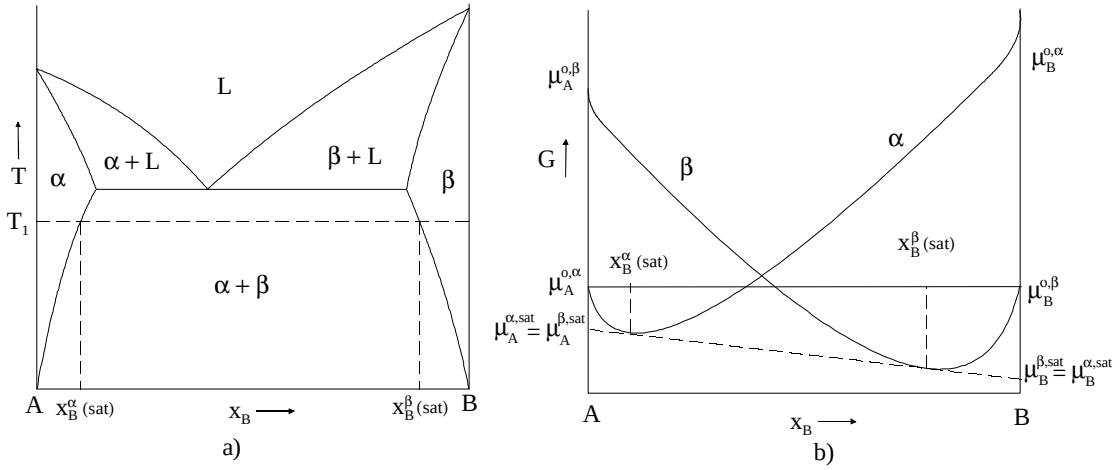

Figure 4: a) Binary phase diagram with limited mutual solubility of components A and B, b) the Gibbs energy diagram at temperature T_1.

A general problem of dealing with solutions thermodynamically can be regarded as one of properly determining the chemical potentials of the components. Usually the treatment utilizes the activity function introduced by Lewis [21], to aid this general problem. Its value lies in close relation to composition; with appropriate choice of reference state the activity approaches the mole fraction as the mole fraction approaches unity. Most commonly it is not the activity which is used but the activity coefficient, which is defined as the ratio of the activity a_i to the mole fraction x_i:

$$\gamma_i = \frac{a_i}{x_i} \tag{4}$$

In terms of the chemical potential the activity can be expressed:

$$\mu_i^j - \mu_i^o = RT \ln a_i^j = RT \ln x_i^j + RT \ln \gamma_i^j \tag{5}$$

where μ_i^o is the chemical potential of pure i in the reference or standard state, μ_i^j the chemical potential of i in phase j, a_i^j the activity of component i in phase j, R is the gas constant, T the temperature, and ($i = A,B,...; j = a,b,...$). In the limiting case of ideal solutions, where the entalphy ($\Delta H_m = 0$) and volume change ($\Delta V_m = 0$) of mixing are zero and the only contribution to Gibbs free energy of mixing arises from the configuration entropy term:

$$\Delta S_m = \sum_{i=A}^{K} x_i \ln x_i \tag{6}$$

the activity coefficient in Eq. (4) is unity and the activity of the component equals its mole fraction (*i.e.* Raoultian behavior). Thus, the activity coefficient represents deviation from ideal behavior.

The values of chemical potentials m_A^j and m_B^j are graphically found at the end-points of the tangents of the curves α and β in the Gibbs free energy plot (Fig. 4(b)). Inside the two phase field the values of the chemical potentials are constant (at equilibrium) and can be found from the tangential points of the common tangent drawn in Fig. 4(b). From the Gibbs free energy diagram at temperature T_1 one can see that when $x_B < x_B^{a(sat)}$, the α-phase is stable since it has the lowest Gibbs free energy and it follows the α-curve up to point $x_B^{a(sat)}$. When the composition is $x_B^{a(sat)} < x_B < x_B^{b(sat)}$, the two phase structure α + β is stable since it has the lowest Gibbs free energy, which now follows the common tangent drawn in Fig. 4 (b) between the points $x_B^{a(sat)}$ and $x_B^{b(sat)}$. Finally, when the composition is $x_B^{b(sat)} < x_B$, the β-phase is stable. In a ternary system, the phase equilibria are obtained by the common tangent-plane construction, where the intersections with the three corners of the diagram represent the chemical potentials. Further details can be found for example from ref. [22].

As only relative values of thermodynamic functions can be determined, an agreed reference state has to be established for each element or species in order to make thermodynamic treatment quantitative. In principle, the choice of the reference state is arbitrary as long as the chosen state is used consequently throughout the analysis. The chosen state is then defined to be zero (in Fig. 4 (b) $m_A^{o,a}$ and $m_B^{o,b}$) and all other possible states of the element are compared against the reference state to obtain their relative stabilities. It should be noted that there are some uncertainties related to the usage of reference states in the literature.

2.2.3 Gibbs free energy change and chemical reaction

If the change in the Gibbs free energy of reaction is negative, the reaction can proceed spontaneously unless there are kinetic barriers that hinder the reaction. The following treatment of the subject follows that of presented in the literature [23]. If one considers a chemical reaction taking place at constant temperature and pressure:

$$aA + bB + ... \; « \; cC + dD + ... \tag{7}$$

where *A, B, C, etc.* are species in the reaction and *a, b, c, etc.* are the moles of the species in question. The Gibbs free energy change *(D_rG)* of the reaction is given by the difference in the chemical potentials of the reactants and the products and is defined as:

$$\Delta_r G = (cm_C + dm_D + ...) - (am_A + bm_B + ...) \tag{8}$$

It is usual to give the Gibbs free energies with respect to the standard states of the species. The standard state of the species taking part in the reaction is the Gibbs free energy of the species in its stable form *(D_rG^o)* [24]. If this is the case equation (8) can be rewritten as:

$$\Delta_r G - \Delta_r G^o = (cm_C + dm_D + ...) - (am_A + bm_B + ...) \tag{9}$$

where D_rG^o is the change in the standard Gibbs free energy of reaction and $m_{A,B,C,D...}$ are the chemical potentials of the species *A, B, C, D....* Substituting from Eq. (5) for $\Delta_r G$ gives:

$$\Delta_r G - \Delta_r G^o = (cRT \ln a_C + dRT \ln a_D + ...) - (aRT \ln a_A + bRT \ln a_B + ...) \tag{10}$$

where *R* is the gas constant, *T* is temperature and the activities *(a_i)* are not equal to one. This can be written as:

$$\Delta_r G - \Delta_r G^o = RT \ln \left[\frac{a_C^c a_D^d ...}{a_A^a a_B^b ...} \right] \tag{11}$$

In the equilibrium state the reactants and products are in equilibrium with each other (*i.e.* $D_rG = 0$) and the activity product given in the brackets is the equilibrium constant K_p:

$$\Delta_r G^o = -RT \ln K_p \qquad (12)$$

This equation signifies that when the reactants in their standard states are transformed into the products in their standard states, the accompanying change in the standard Gibbs free energy, $D_rG°$, is equal to $-RTlnK_p$, where K_p is related to the activities at the equilibrium concentrations. If all the reactants and the products are gaseous, then K_p is a function of temperature only, because the corresponding $D_rG°$ is a function of temperature alone. However, if one or more of the reactants or the products are condensed phases, K_p and $D_rG°$ are dependent on pressure as well as temperature according to the definition of standard states. In general, the effect of a few bars of pressure on condensed phases and on their $G_i°$ is negligibly and thus K_p is frequently considered to be independent of pressure. It should be noted that the change in the Gibbs free energy is also related to the corresponding changes in the enthalpy and the entropy according Eq. (1). The D_rG for a reaction is found usually by adding the Gibbs free energies of formation (from pure stable elements), $\Delta_r G^o$, of the products and subtracting that of the reactants according to the Hess' principle [25]. The thermodynamic data for the calculations can be found for example from ref. [26].

2.2.4 The phase rule and phase diagrams

The phase rule defines the condition of equilibrium in a heterogeneous system by the relation between the number of co-existing phases *p*, number of components *c* and the number of degrees of freedom *f* as follows:

$$p + f = c + 2 \qquad (13)$$

The number 2 in Eq. (13) represents pressure and temperature. The number of degrees of freedom of the equilibrium state is the number of conditions (variables) that must be fixed in order to define the corresponding state. It is assumed that temperature, pressure and composition are the only variables that can influence the phase equilibria. For

example the effect of surface-tension forces at the boundaries between phases, of gravitational fields, magnetic fields, stresses *etc.* is considered to be of negligible importance. In many cases the pressure is assumed to be fixed and the phase rule reduces to:

$$p + f = c + 1 \qquad (14)$$

Phase diagrams are graphical representations of the domains of stability of the various classes of structures (one phase, two phase, three phase *etc.*) that may exist in a system at equilibrium. Phase diagrams are most commonly presented in the temperature - pressure-composition space. In the context of this thesis, only systems where the pressure variables can be neglected are considered (as the binary A-B phase diagram in Fig. 4 (a)). Many other coordinate systems, for example activity of one component versus mole ratio of the others, are also possible [27].

To represent the phase equilibria in ternary system at constant pressure, a three-dimensional construction is required. However, as many practical processes are carried out at constant temperature, the most quantitative ternary phase diagrams are presented as isothermal sections at certain temperatures. The most common method for plotting composition in a ternary system uses an equilateral triangle, sometimes referred as the Gibbs triangle. As an example, the ternary Si-Ta-Cu phase diagram from the Publications I and II used to study phase relations in the Si/Ta/Cu metallization system is shown in Fig. 5. At the corners are the pure elements Ta, Si and Cu and the three edges represent the Cu-Si, Ta-Si and Cu-Ta binary systems. There are no ternary phases in this system. Triangles in the diagram, bounded by three straight lines, represent three phase equilibrium, such as Cu+$TaSi_2$+Ta_5Si_3 in Fig. 5. Two tie-lines can not cross each other, since at the point of intersection there would be four phases in equilibrium and this would violate the Gibbs phase rule (at a chosen temperature: $f = c(=3) - p(=4) = -1$).

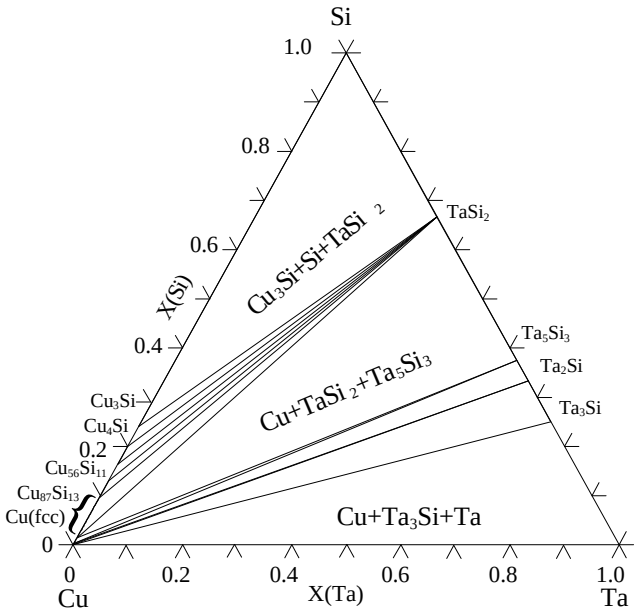

Fig. 5. Isothermal section at 973 K from the evaluated ternary Si-Ta-Cu phase diagram.

2.2.5 Calculation of phase diagrams

Phase diagrams are often regarded as something that can only be determined experimentally. However, as phase diagram is the manifestation of the state of equilibrium, it is possible to construct any kind of phase diagram if the equilibrium state of the system has been calculated. This in turn requires the evaluation of the thermodynamic properties of the corresponding system by assessing all the available experimental information in thermodynamic terms. Generally one is interested in equilibria under constant pressure and therefore the Gibbs free energy is the expedient thermodynamic function. Analytical expressions for the free energy functions of all phases must be derived first. The thermodynamic models used in the description of the Gibbs free energy of different phases are important, since successful and reliable calculation relies on the appropriate choice of model for each phase appearing in the system. Then by summing up all the Gibbs free energies of individual phases, the phase equilibria can be computed by minimizing the total Gibbs free energy of the system. The matemathical expressions for the Gibbs free energy of the individual phases contain parameters which have to be optimized to give the best fit to all the experimental information available. A major difficulty arises from the fact that the value of a parameter

(which is used in the description of a simple system) will affect the evaluation of all the related higher systems. Thus, one should use as much information as possible from different sources in each optimisation process. The preceding approach is known as the CALculation of PHAse Diagrams (CALPHAD) method [24,28].

The CALPHAD method is based on the axiom that complete Gibbs free energy versus composition curves can be constructed for all structures exhibited by the elements right across the whole alloy system. This involves the extrapolation of *(G,x)*-curves of many phases into regions where they are metastable (see Fig. 4 (b)) and, in particular the relative Gibbs free energies for various crystal structures of the elements of the system must therefore be established. These are called as lattice stabilities and the Gibbs free energy differences between all the various potential crystal structures in which an element can exist need to be characterized as a function of temperature, pressure and volume [24,28].

CALPHAD method is commonly used for evaluating and assessing phase diagrams. The power of the method is clearly manifested in its capability to extrapolate higher order systems from lower order systems, which have been critically assessed, thus reducing the number of experiments required to establish the phase diagram. The determination of binary equilibrium diagrams usually involves the characterization of only a few phases, and experimental thermodynamic data on each of the phases is generally available in various thermodynamic data banks as well as in the literature. However, when handling multicomponent systems or/and metastable conditions there is a need to evaluate the Gibbs free energies of many phases, some of which may be metastable over much of the composition space. Readers interested in the actual thermodynamic modelling procedures and issues and problems associated with them are referred to vast amount of available literature, for example review articles and books [24, 28-30]. In this thesis the CALPHAD method has been applied in the extrapolation of ternary phase diagrams from the assessed binary thermodynamic data. It should, however, be emphasized that it is not possible to determine ternary phase diagram solely based on the data on binary phase diagrams, since the binary data do not yield

information about ternary interaction parameters. Therefore, experimental work is always required in the critical assessment of phase diagrams as discussed above.

Phase diagrams are useful for concisely presenting the equilibrium relationships in alloy systems. However, since phase diagrams are equilibrium diagrams they do not provide any information on reaction rates, on the effect of defects or on the phase distribution and morphology. Nevertheless, because the equilibrium diagrams are directly related to free energy versus composition diagrams, information about the driving forces of different reactions in the system can be obtained from the *(G,x)*-diagrams. It is also possible to describe metastable phases with the help of *(G,x)*-diagrams and establish relative stabilities of the phases.

In order to take into account reaction rates *etc.* one needs to bring kinetics into the analysis. Therefore, thermodynamic data of the system must be combined with the available kinetic data to provide information about time dependence and reaction sequences during phase transformations. Even so, it is to be noted that thermodynamics provides the basis for the diffusion kinetics as well.

2.3 Kinetic properties

Thermodynamics provides the basis for analyzing reactions between different materials. However, one cannot predict the time frame of the reactions on the basis of the phase diagrams. Therefore, diffusion kinetics must be brought into the analysis. In this section the basics and some of the related nomenclature of solid state diffusion are introduced. For a thorough treatment of the theory of diffusion reader is referred to excellent treatises on the subject [31-33]. Relations between different diffusion coefficients as well as experimental techniques to obtain numerical values for the diffusion coefficients are presented in refs. [34-39].

2.3.1 Atom movements

Reactions in and between solids involve diffusion in the solids or across the interfaces. The movement of atoms necessarily requires a driving force, which can be thermal, chemical, electrical or mechanical in origin. The chemical diffusion in materials is most commonly described with the help of the Fick's I and II laws, where the driving force is provided by the concentration gradient [31-33]. Solid state diffusion phenomena are divided into two major categories: volume or bulk diffusion and short-circuit diffusion. Volume diffusion is further divided into two categories: interstitial diffusion and substitutional diffusion mediated by vacancies. An atom is said to diffuse interstitially when it passes from one interstitial site to one of its nearest-neighbor interstitial sites without permanently displacing any of the matrix atoms. Small atoms, such as H, C, O, and N, can diffuse by this mechanism. At high temperatures, the volume diffusion is usually predominant in metals. However, at relatively low temperatures with respect to melting points of the corresponding materials (with metals 0.3-0.5 T_m [40]) short-circuit diffusion (5 to 6 orders of magnitude faster than the volume diffusion at 0.5 T_m) is important mechanism [41] (Fig. 6).

In order to be able to analyze correctly the available diffusion data it is important to recall some additional criteria concerning the values of diffusion coefficients in pure metals [40]:

(1) The (self) diffusion coefficient at the melting temperature D_{T_m} is order of 10^{-8} cm^2/s (0.5×10^{-8} for face centered cubic (fcc) and 3×10^{-8} for body centered cubic (bcc))
(2) The activation energy (Q) scales with the melting temperature (T_m): $Q/RT_m \approx 17$
(3) The pre-exponential term (D_0) is close to 1 cm^2/s (0.3 in fcc and 1.6 in bcc)
(4) The ratio of activation energies for short-circuit and volume diffusion (Q_{gb}/Q_v) ranges between 0.5 – 0.7 at 0.5 T_m

The significance of the magnitude of the diffusion coefficient lies in the quantity $\sqrt{Dt}$, characterized as the "diffusion length". This quantity describes a mean diffusion distance in terms of diffusion time [32]. It is to be noted that diffusion coefficients in solids have a strong exponential dependence on temperature (*i.e.* according to the Arrhenius law). Further, it should be emphasized that diffusion coefficients in metals are usually anisotropic and are dependent on the crystal direction. Moreover, when considering ordered compounds, like silicides, one should recognize that ordering always renders diffusion more difficult. The basic reason behind this behavior is the progressive creation of two (or more) distinct sub-lattices for unlike atoms, which makes random motion of a vacancy more difficult [41].

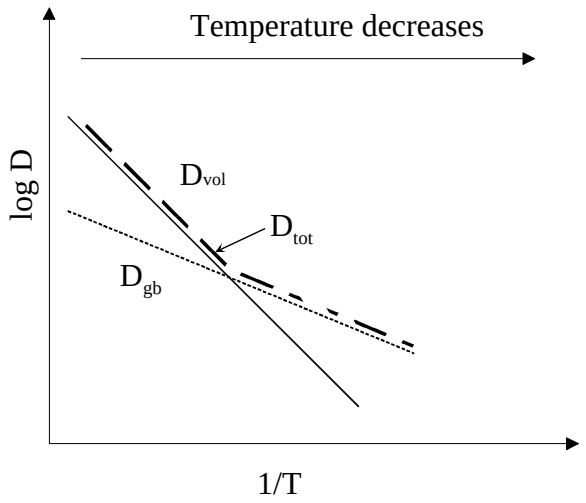

Figure 6. Contribution of grain boundary diffusion coefficient D_{gb} and the volume diffusion coefficient D_{vol} to the total effective diffusion coefficient D_{tot} as a function of temperature.

2.3.2 Interdiffusion and intrinsic diffusion coefficient

By assuming a local equilibrium situation and that there are no nucleation problems, the number and composition of phases that will grow in a binary diffusion couple can be predicted from the phase diagram. Since the motion of different atoms in crystal lattice is relative, the chemical diffusion in solids has to be fixed to a certain frame

of reference. The frame of reference, which is chosen for the description of the interdiffusion process, determines the definition of the evaluated diffusion coefficients.

Most commonly the interdiffusion flux equations, related to the Matano frame of reference fixed to the ends of the sample, are used. In the case of a constant total volume the interdiffusion coefficient $\tilde{D}(c_i^*)$ at a certain concentration can be determined from the penetration plot of c_i versus l by using the Matano-Boltzmann equation [32-35]:

$$\tilde{D}(c_i^*) = -\frac{1}{2t}\left(\frac{dl}{dc_i}\right)^* \int_{C_i^-}^{C_i^*} l\,dc_i \qquad (15)$$

where l is the distance, c_i is the concentration of component i and t is the time. From the same concentration profile the position of the Matano plane can be graphically determined [34,35]. The determination of the Matano plane from the penetration profile of a binary diffusion couple is shown schematically in Fig. 7. The Matano reference plane $l_o = 0$ is defined in such a way that the hatched areas in Fig. 7 are equal.

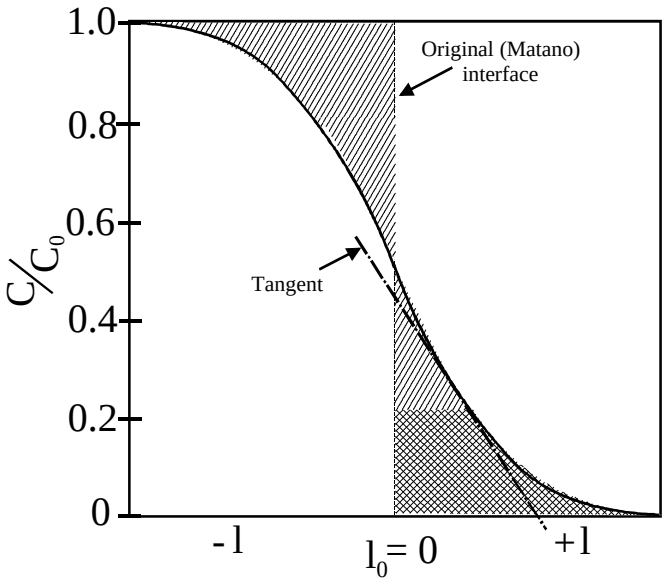

Fig. 7. Determination of the Matano interface from the concentration profile.

The thicknesses of the phases formed in the diffusion couple are directly related to the interdiffusion coefficients in the phases. If the coefficients and the composition limits are known, the layer thicknesses of the phases in the diffusion zone between two solids A and B can, in principle, be calculated. The necessary conditions for the analysis are that the local equilibrium is established (this is further discussed in Chapter 2.3.4) and consequently that diffusion through the layers is the rate limiting step. When diffusion is the rate-determining step, one is operating in the parabolic growth regime. On the other hand, if interfacial reactions are the rate-controlling step, the corresponding growth regime is linear. Further discussion about different regimes of growth and related issues such as the critical thickness of a growing phase, can be found for example from refs. [42-49].

The interdiffusion coefficient $\tilde{D}$ can be seen as a measure of mixing rate during the interdiffusion in a couple and it usually depends on the concentration. The same interdiffusion coefficient $\tilde{D}$ can be used for the description of the diffusion behavior of both species. It does not give any information about the individual mobilities of the diffusing species. If the real - or intrinsic - diffusivities (D_i) of both components have to be investigated, the diffusion fluxes relative to some lattice plane in a phase have to be known. The origin of this so-called Kirkendall frame of reference can be found in a single phase diffusion couples by using inert markers situated at the original contact interface at $t = 0$. The unequal diffusion fluxes of the components with respect to the lattice planes in a phase is compensated by a flux of vacancies in the same direction as the flux of the slower component. The intrinsic diffusion flux is usually given with respect to the above-defined Kirkendall frame of reference as [34]:

$$J_i^K = -\frac{D_i}{V_m}\frac{dx_i}{dl} \qquad (16)$$

where the superscript K refers to the Kirkendall frame of reference, D_i is the intrinsic diffusion coefficient of the component i, V_m is the molar volume, x_i the mole fraction of

the component *i* and *l* the distance. The sum of the intrinsic fluxes of all the components equals zero:

$$J_A^K + J_B^K + J_V^K = 0 \qquad (17)$$

As diffusion proceeds the Kirkendall plane moves with respect to the Matano plane with certain velocity $v^{K/M}$. This velocity can be defined for each lattice plane in the diffusion zone, but can only be measured "easily" at the lattice plane corresponding to the original interface at $t = 0$ by the relation:

$$v^{K/M} = \frac{\Delta l}{2t} \qquad (18)$$

where *Dl* is the marker displacement, *i.e.* the distance between the Kirkendall plane l_K and the Matano plane $l_o = 0$. The intrinsic diffusion coefficients D_i are related to $v^{K/M}$ and the interdiffusion coefficient $\tilde{D}$ by the relations:

$$v^{K/M} = V_A\left(D_A - D_B\right)\frac{\partial c_A}{\partial l} \qquad (19)$$

$$\tilde{D} = c_A V_A D_B + c_B V_B D_A \qquad (20)$$

where c_i is the concentration of a component *i* and V_i is the partial molar volume of a component *i*.

2.3.3 Thermodynamic factor in diffusion coefficients

Fick's first and second laws for the material transport have limited validity from a fundamental point of view. Deviations from the Fick's laws have been observed in several ternary systems, for example "up-hill" diffusion of a component against its own concentration gradient [50-53]. Onsager postulated the phenomenological equations for

all transport processes stating that each thermodynamic flux is linearly related to every thermodynamic force [32,33]. Diffusion of matter takes place in a system on account of the striving for the state of minimal energy. Therefore, the actual driving force behind the chemical diffusion process is the gradient of the chemical potential. In the absence of any other driving forces, the flux of A atoms in a binary system AB can be written as:

$$J_A = -L_A \frac{\partial m_A}{\partial l} \tag{21}$$

where the L_A is the phenomenological coefficient related to the intrinsic diffusion coefficient D_A. As the chemical potential is related to the activity through Eq. (5) and the activity is related to the atomic fraction x_i through Eq. (4) it can be shown that [35]:

$$D_A = \frac{V_m L_A RT}{V_B c_A}\left[1 + \frac{\partial \ln g_A}{\partial \ln x_A}\right] \tag{22}$$

In the case of autodiffusion of tracer A* in A, it is reasonable to assume an ideal solution behavior, since isotopic effects are negligible. This means that the thermodynamic term in brackets in Eq. (22) is 1 and the equation becomes:

$$D_A^* = \frac{L_A RT}{c_A} \tag{23}$$

Combining Eqs. (22) and (23) one obtains the relation between the tracer and the intrinsic diffusion coefficient:

$$D_A = D_A^*\left[1 + \frac{\partial \ln g_A}{\partial \ln x_A}\right] \tag{24}$$

2.3.4 Multiphase diffusion and reaction kinetics

Generally, in a binary system the interaction between components and the resulting reaction products can be predicted by using the relevant phase diagram. After annealing at certain temperature for sufficiently long time, all the thermodynamically stable phases of the system at that particular temperature (and only them), will exist as layers between the end members. According to the phase rule only single phase homogeneous regions can be formed, the interfaces between various phases must be macroscopically planar, and the concentrations at the interfaces of various phases can be read from the phase diagram. What has been stated above requires necessarily that there are no nucleation problems associated with the phase formation and the diffusion is the rate-limiting step. This will ultimately lead to the phase sequence determined by the corresponding phase diagram. In principle, in a specific binary system one can also say something about the temporal evolution of the system, if the interdiffusion coefficients in all the appearing phases are known. However, when one is dealing with higher order systems the prediction of the reaction layers becomes much more difficult. In a ternary system the additional degree of freedom enables also the formation of two phase regions and curved interfaces. This means that theoretically many different phase sequences are possible and the final structure cannot be, in general, interpreted directly from the phase diagram. In addition, the concentration and activity gradients are not necessarily always into the same direction as in the binary systems, thus enabling for example the above mentioned "up-hill" diffusion.

Phase transformation will be diffusion controlled when the mass transport through the bulk is the rate-limiting step. Then the boundary conditions governing the rate of diffusion can be evaluated by assuming that whenever two phases meet at the interface, their compositions right at the interface are very close to those required by the equilibrium, and the thermodynamic potentials are continuous across the interface. This is called the local equilibrium approximation [30]. If the local equilibrium can be assumed in the system, it is often possible to use phase diagrams coupled with few rules to predict possible or at least to rule out impossible reaction sequences in ternary systems.

The first rule is concerned with the principle of mass-balance, which requires that material can not be created or destroyed during reaction. This requires that the diffusion path, which is a line in the ternary isotherm, representing the locus of the average compositions parallel to the original interface through the diffusion zone [54-56], crosses the straight line connecting the end members of the diffusion couple at least once. During the reaction, the system will follow only one unique, reproducible diffusion path. Kirkaldy *et.al.* have presented number of rules which the diffusion path must obey [54-56].

The concept of diffusion path can be comprehended with the help of Fig. 8, which shows the hypothetical A-B-C phase diagram with two binary compounds X and Z and the ternary compound T [34]. In Figure 8 four diffusion paths are given with the corresponding morphologies of the diffusion zone, for the diffusion couple C versus X. They all fulfill the mass-balance requirement. This also gives constraints about the relative thicknesses of the various diffusion layers like T and Z in Fig. 8 (b). The Z-phase has to be much thinner than the T-phase in order to comply with the mass-balance. This is because the Z-phase is much further from the contact-line (*e.g.* average composition) than the T-phase. Not only the relative thicknesses, but also the total thickness of the diffusion layer is related to the diffusion path. If *e.g.* in the Z-phase the diffusion is very slow and in the T-phase fast, then the total layer width for Figs. 8 (b) or (c) will be smaller than in the case of Fig. 8 (d). In the first examples, the continuous Z-layer acts as a kind of diffusion barrier, whereas in the latter case the total layer thickness is governed by the faster diffusion in the T-phase, which is probably only little hindered by the discontinuous Z-particles. One must realize that diffusion path corresponds only to a topological distribution of phases in space.

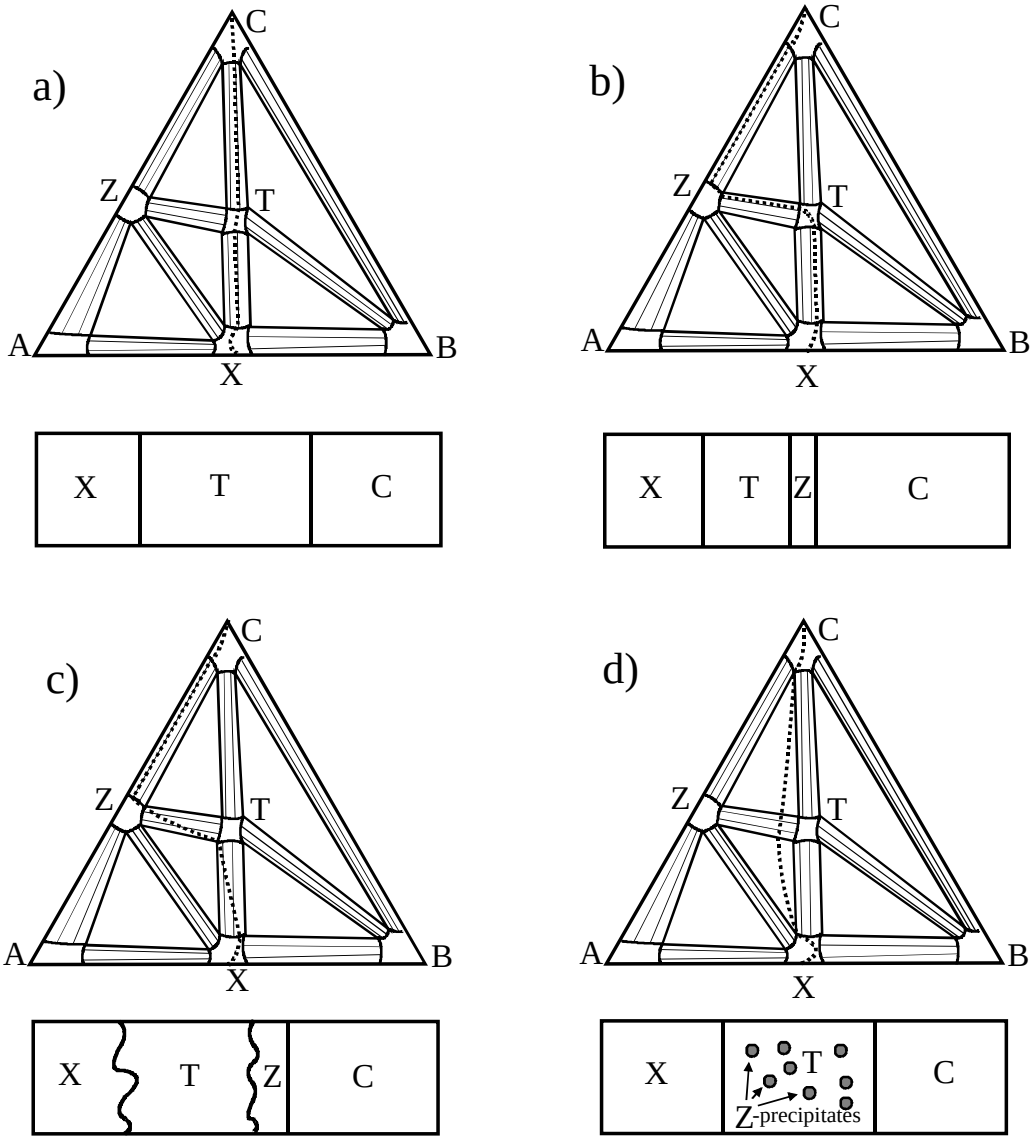

Figure 8. Examples of possible morphologies for the reaction layer in a diffusion couple X/C. The corresponding diffusion paths are plotted on the isotherms [34].

It is difficult to predict the diffusion path or to exclude impossible ones with the help of the mass-balance requirement alone. Thus, van Loo *et.al.* [34] have introduced another rule, which is based on the thermodynamic driving force behind the diffusion phenomenon. The rule states that no element can diffuse intrinsically against its own activity gradient. If this would take place, it would mean that atom should diffuse from low chemical potential area to high chemical potential area - a process that does not

spontaneously occur in nature. By calculating the chemical activities of components as the function of the relative atomic fractions of the elements, and taking into account the above mentioned mass-balance considerations, the sequence of compounds formed during reaction can often be predicted as can be seen from the following examples.

An example from the literature is shown in Fig. 9, which is redrawn from ref. [57]. It shows the isothermal section from the Cr-Si-C system at 1273 K. The experimentally determined diffusion path is superimposed into the isothermal section and into the activity diagram. The activity diagram shown in the right-hand side of Fig. 9 is one form of many different types of stability diagrams. In such a diagram the thermodynamic potential (or activity a_i) of one of the components is plotted as a function of relative atomic fractions of the other two components. The activity values needed can be calculated from the assessed thermodynamic data. When calculating the activities of the components, the activities of the stoichiometric compounds at equilibrium are regarded to be one. It should be noted that the precision of the calculations is very much dependent on the accuracy and consistence of the thermodynamic data used. Therefore, great care should be exercised when using data from different sources.

In activity diagrams the stoichiometric single phase regions are represented as vertical lines, two phase regions as areas and three phase fields as horizontal lines. The vertical left and right hand axes represent the binary edge systems. From Fig. 9 it is evident that Cr moves along its decreasing activity in the experimentally observed reaction sequence SiC/τ/Cr_3Si/Cr_3Si+Cr_7C_3/Cr_7C_3/$Cr_{23}C_6$/Cr. The phase sequence SiC/Cr_3C_2/τ/CrSi/Cr_5Si_3/Cr_3Si/Cr, another example of a diffusion path that fulfills the mass-balance requirement, is impossible from the thermodynamic point of view, since Cr would have to diffuse against its own activity gradient inside the ternary phase τ to get from CrSi to Cr_3C_2.

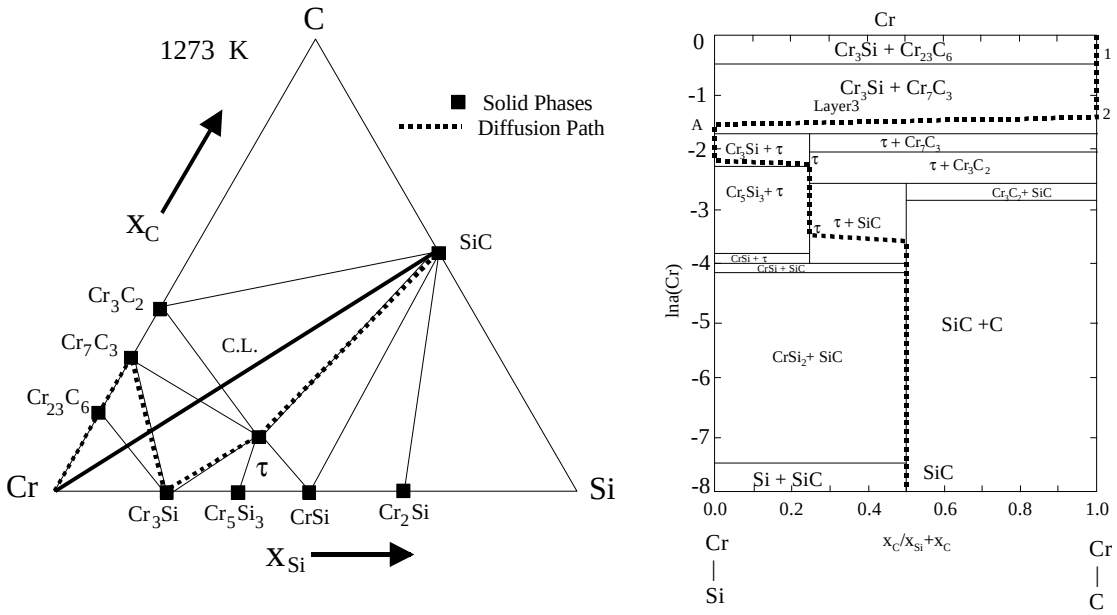

Figure 9. Experimentally determined isothermal section and the calculated activity diagram at 1273 K. The contact line (C.L.) and the diffusion path are also superimposed onto both diagrams. τ is the ternary phase.

Another example is from the Si-Ta-C system that was used in this thesis to investigate reaction between the TaC layer and the Si substrate (Figs. 10 and 11). In Fig. 10 the isothermal section from the Si-Ta-Cu ternary phase diagram is presented. The initial situation Si/TaC is presented as the contact line (C.L.) in Fig. 10. The TaC/Si interface is not stable and therefore mass transport starts to take place in the system during the annealings. With the help of the calculated activity diagrams for Si and Ta, it can be seen that for example the sequence Si/SiC/$TaSi_2$/TaC is possible according to the activity diagrams and the phase diagram (Figs. 10 and 11). Both elements, Ta and Si, can move along their lowering activity gradients in this reaction sequence and diffusion of both elements in the reaction is therefore allowed on the thermodynamic grounds. Despite the fact that there exists a TaC + $TaSi_2$ two phase region in the phase diagram (Fig. 10), SiC must be formed to incorporate the carbon released after the formation of $TaSi_2$, because of the mass-balance requirement. The sequence predicted above was experimentally verified to form after the annealings [58].

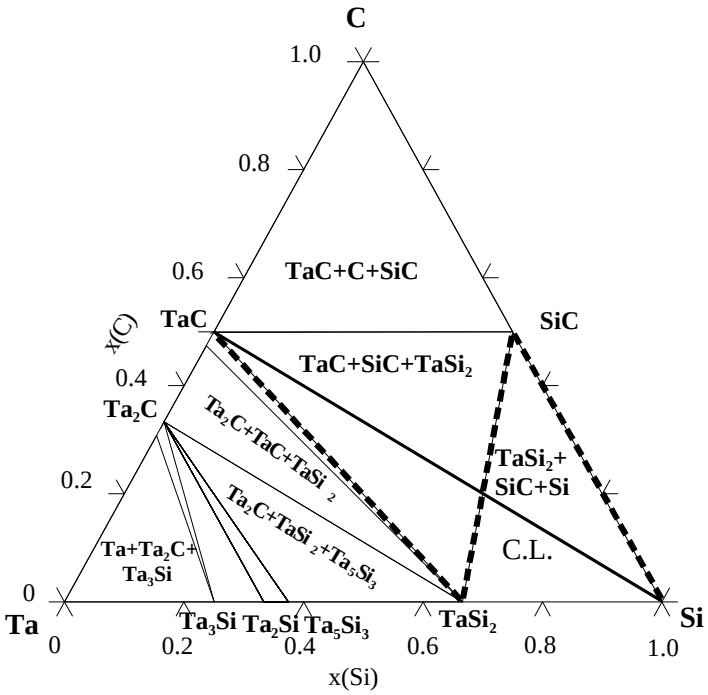

Figure 10. Isothermal section from the evaluated ternary Si-Ta-C phase diagram at 1073 K. The hypothetical diffusion path is also superimposed into the isothermal section.

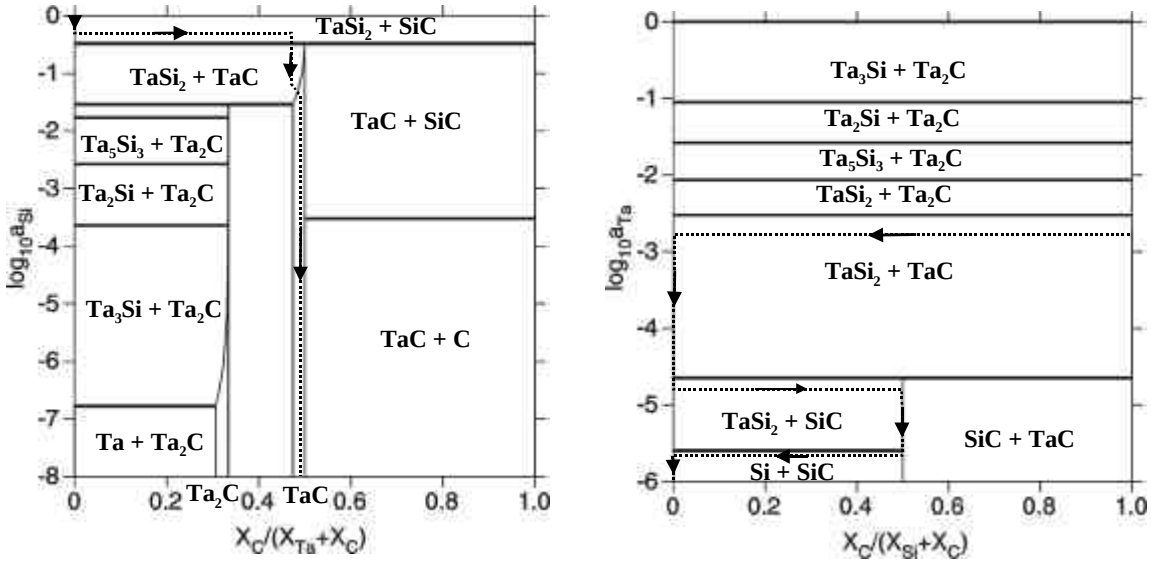

Figure 11: a) Potential diagram ($\log_{10}a_{Si}$ vs. $x_C/x_{Ta}+x_C$) and b) ($\log_{10}a_{Ta}$ vs. $x_C/x_{Si}+x_C$) for Si-Ta-C system at 1073 K with the superimposed diffusion path.

It should be noted that in thin film samples (as when working with very thin diffusion barriers) the assumption of local equilibrium, which is necessary for the above treatment, is not self-evident. The assumption of local equilibrium requires that reactions at the interfaces are fast enough so that all the atoms arriving in the reaction region are used immediately and the rate-determining step is diffusion, as discussed above. However, with very thin layers this requirement may not be fulfilled. The reasons for this originate mainly from special conditions prevailing during thin film reactions: (a) relatively low reaction temperatures, (b) small dimensions, (c) high density of short-circuit diffusion paths, (d) relatively large stresses incorporated in thin films, (e) relatively high concentration of impurities, (f) metastable structures, (g) large gradients, and so on. These conditions mean that the complete thermodynamic equilibrium is hardly ever met in thin film systems. However, the local equilibrium is generally attained at interfaces quite rapidly. Therefore, the procedure presented above provides a feasible analysis method also for studying thin film reactions.

2.3.5 The role of grain boundaries

Thin films possess usually high density of grain boundaries (Fig. 12), which can have effect on the growth kinetics. This is because of the enhanced atom transport via the short-circuit paths. A simple situation readily occurs in thin film experiments: columnar grains, with their long axis along the direction of the diffusion flux. This situation can be modeled by dividing the film into two different parts: one with diffusion coefficient D_{vol} (lattice) and the other with diffusion coefficient D_{gb} (grain boundary). The number of atoms transported per unit area and unit time is given by:

$$M(t) = (A_l J_l + A_{gb} J_{gb}) = (A_l D_{vol} + A_{gb} D_{gb}) \frac{dc}{dx} \qquad (25)$$

where A_l and A_{gb} are the cross-sections of the grains and the grain boundaries per unit area.

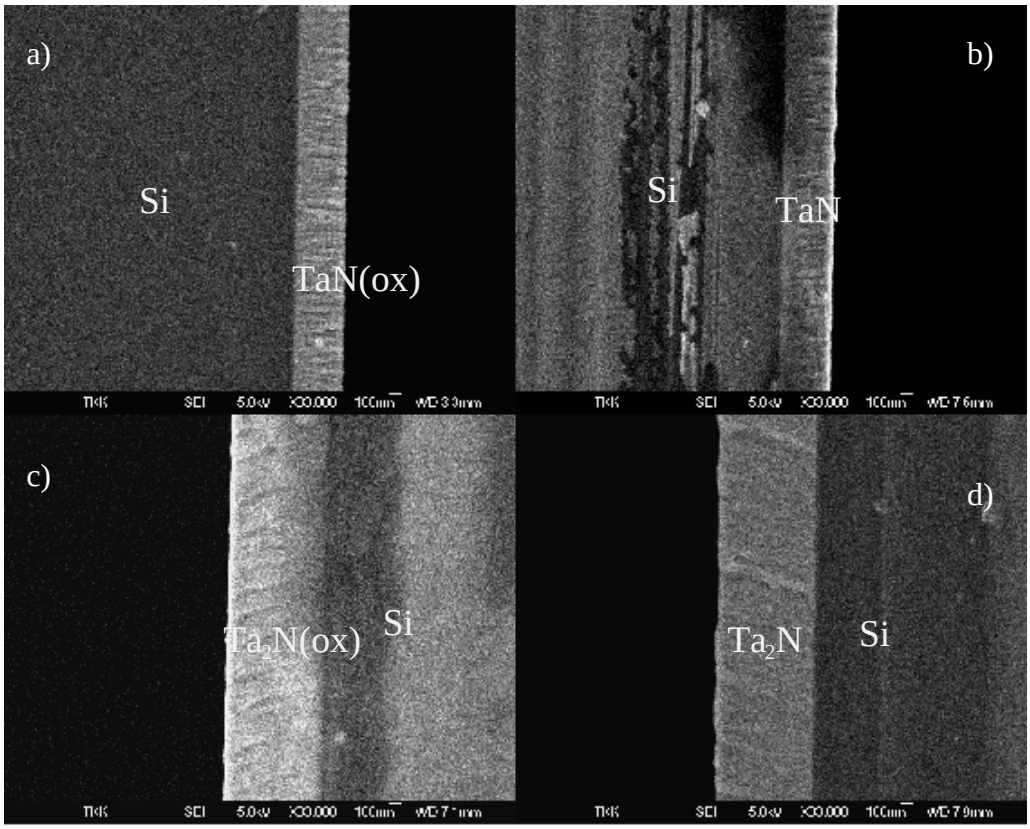

Figure 12. Cross-sectional SEM-micrographs of as-deposited (a) TaN on SiO_2/Si, (b) TaN on silicon c) Ta_2N on SiO_2/Si and d) Ta_2N on silicon showing columnar microstructure. Micrographs are in the same scale and scale bar length is 100 nm.

With conventional thickness d of grain boundaries, $A_l \approx 1$ and $A_{gb} \approx 2d/d$, where d is the average grain diameter [59]. Instead of the lattice diffusion constant D_{vol}, the effective diffusivity D_{tot} must now be considered:

$$D_{tot} = D_{vol} + \frac{2D_{gb}d}{d} \qquad (26)$$

Thus, the value of the diffusion "coefficient" has increased. This may also influence the regime of layer growth, in particular if the thickness of the film is small. Short-circuit diffusion may enhance the atom transport to such an extent that the reaction(s) at the

interfaces become rate-limiting. More thorough treatment of short-circuit diffusion may be found for example in reference [60].

2.3.6 Role of impurities

Impurities have important effects on the formation of phases in thin film and bulk couples. Presence of some impurity may enhance the formation of a particular phase at the expense of another. Impurities may increase or decrease reaction temperatures or influence the kinetics of a phase transformation. Impurities are also frequently responsible for the absence of phases in diffusion couples as compared to the corresponding phase diagram. One example of the increased reaction temperature is the formation of $TaSi_{2,}$ in the reaction between thin Ta film and Si substrate, which occurs at 923 K [61]. However, if there is oxygen at the Si/Ta interface the temperature of formation will rise well above 1023 K [62]. Another example of bulk samples is the catalyzing effect of phosphorous on the formation of Cu_3Si in the reaction between bulk copper foil and Si substrate [63]. The effect of impurities on diffusional transport should also be considered. Impurities may segregate preferably to grain boundaries and interfaces. When they segregate to grain boundaries they may reduce the effect of the short-circuit diffusion paths, thus affecting the mass transport in the system.

2.4 Microstructural properties

For a new phase to form, at least two factors are required: the thermodynamic driving force and the mobility of atoms. The latter is strongly depended on the microstructures of the materials taking part in the reaction. As has been mentioned, thin film structures typically possess very high density of grain boundaries. These more or less disordered regions offer high diffusivity paths for the atoms. This is clearly denoted when thin film metallisations have columnar structures, which are often observed after physical vapor deposition (PVD). Thus, it would be beneficial to somehow eliminate these short-circuit diffusion paths. This can be achieved for example by blocking the

grain boundaries with impurity atoms/compounds or by producing an amorphous structure.

The driving force for the equilibrium segregation of solute or impurity atoms to grain boundaries is systems tendency to lower its total free energy. In addition to kinetic constraints the extent of intergranular segregation depends on impurities influence on the grain boundary energy as well as on the factors controlling their solubility, *i.e.* size factor and chemical interactions between dissimilar atoms. Since both the kinetics and the solubility depend on temperature, the segregation of impurities decreases with increasing temperature. By gathering large amounts of experimental data on grain boundary segregation Hondros and Seah [64] showed that the smaller the solubility of an impurity in the solvent the higher is its segregation potential. This “rule of thumb” is frequently used when considering the segregation tendency of a given impurity.

Because of the analogies between intergranular segregation and adsorption at free surfaces, classical free surface adsorption models have often been used for evaluating grain boundary segregation [65]. This approach is valid if it takes into account the specific features, which differentiate the grain interface from surfaces. Thus, even the most dilute grain boundary can be regarded as a two dimensional phase with the same components as in the bulk [66]. It is to be noted that the equilibrium condition, *i.e.* that the chemical potential of a component *i* has the same value in all phases of the system, is valid also for grain boundaries and surfaces. Several treatments of intergranular segregation have been published during the past decades. Extensive reviews of the models can be found from refs. [64, 65].

Elimination of high diffusivity paths can also be achieved by amorphisation of the crystal structure [67-70]. It is generally thought that absence of grain boundaries slows down diffusion of all elements through barrier layer. However, since structure is not ordered there should be more free space in amorphous materials for atoms to squeeze between others than in crystal. Thus, “volume” diffusion in amorphous materials is generally much faster than in crystalline media. Nevertheless, in thin film samples grain

boundary density is usually so high that elimination of grain boundaries is anticipated to be advantageous. It is to be noted that the detailed mechanisms of diffusion in amorphous alloys are not presently well understood [8,71].

In thin film technology there has recently been considerable advances in producing metastable and amorphous films resulting from the development of the physical vapor deposition (PVD) techniques, especially magnetron sputtering. During sputter-deposition, the atoms condensing in an intermixed state try to find a stable configuration [72]. Structural order in a coating is produced largely by the mobility of the adatoms. Low mobility does not allow the formation of equilibrium phases and metastable and/or amorphous phase formation is likely. Therefore phase formation and crystalline state is mainly influenced by substrate temperature together with surface and bulk diffusion [73]. It should also be noted that it is easier to form amorphous structures with mixtures/compounds than with pure elements.

Amorphous films are, however, always metastable. For an amorphous material of given composition, there always exists a crystalline phase or mixture of several crystalline phases which are thermodynamically more stable than the amorphous phase. In other words, amorphous phases exist only because nucleation or/and growth of equilibrium phases is prevented. Thus, there is generally a considerable large driving force for the crystallization of the film. Nevertheless, it is known that transition metals can be stabilized in their amorphous forms by adding metalloids (*e.g.* B, C, N, Si, and P) [74]. This concept has been used for example in the case of TaSiN films. The addition of Si into TaN film resulted into an amorphous structure, which did not crystallize easily [67-70].

The crystallization temperature of the amorphous film is perhaps the most important parameter, which determines the effectiveness of the barrier layer. It has been experimentally found that the presence of copper overlayer enhances the crystallization of some underlying amorphous films [67]. As amorphous films are commonly treated as undercooled liquids, one may think that copper, which diffuses into the amorphous layer,

offers heterogeneous nucleation sites for the crystallites to form, thus reducing the critical nucleus size, which is required for the formation of a stable crystal.

2.5 Diffusion barriers in literature

The most frequently proposed diffusion barriers for copper metallization are based on refractory metals, such as Ti and Ta, as well as their binary nitrides and carbides, and ternary TaSiN and TiSiN compounds. The binary compounds rely on their excellent stability. The ternary films can also be classified in the same category, but their unique property is the amorphous structure, which is produced in order to slow down the diffusion processes in these barriers. There are naturally also numerous other suggestions; some of them are summarized in Table 1.

Table 1. Summary of the studies involving the Si/barrier/Cu structures based on ref. [75]. The list has been expanded to contain also some interesting results about Ta-based diffusion barriers published after 1993.

Sample configuration (nm)	Annealing ambient	Barrier effective at (min/K)	Phase formation (min/K)
Si/$Ti_{55}N_{45}$(95)/Cu(175)	N_2	0.5/973	Cu_3Si 0.5/973
Si/$Ti_{45}N_{55}$(120)/Cu(175)	N_2	0.5/1173	Cu_3Si 0.5/1173
Si/$TiN_{0.95}$(50)/Cu(65-200)	Vacuum	60/873	At higher temperature, the degradation earlier for Si/TiN/Cu than for Si/TiN(O)/Cu
Si/$TiN_{1.3}O_{0.75}$(50)/Cu(65-200)	Vacuum	60/873	
Si/$Ti_{52}N_{48}$(55,Sputtered)/Cu (250)	Vacuum	30/973	Small Cu-Si nodules at 973
Si/TiN(60, CVD)/Cu(250)	Vacuum	30/823	Small Cu-Si nodules at 873
Si/TiN(40-60,CVD)/ Cu(250)	Vacuum	30/ <773	Cu-Si compounds at 798

Sample configuration (nm)	Annealing ambient	Barrier effective at (min/K)	Phase formation (min/K)
Si/$W_{76}N_{24}$ (120,amorphous)/Cu(620)	Vacuum	30/1023	30/1073 W_5Si_3
Si/$W_{46}N_{54}$(120, polycrystalline/Cu(620)	Vacuum	30/973	30/1023 W_5Si_3
Si/Ti/Cu	Vacuum	…	Reaction at 40/773
Si/Ti(220)/TiN(100)/ Cu(160)	Vacuum	30/973	Reaction at 40/773
Si/TiN(100)/Cu(160)	Vacuum	30/973	Reaction at 40/773
Si/W_2N(150)/Cu(50-100)	He	30/773	
Si/Ta(50)/Cu(100)	He	3 ^{0}C/min to 933	Ta out-diffuses to Cu surface before any interaction at 1023
Si/Ta(20)/Cu(150)	Ti purified He		593 by diffusion of Cu through Ta
Si/Pd(100)/Cu(200)	N_2:H_2 =9:1	30/473	Reaction at 30/573
Si/W(100)/Cu(200)	Vacuum	…	Cu diffuses through W gb's at 30/450
Si/Cr(20)/Cu(200)	Vacuum	…	Limited Cu diffusion in Si at 30/723
Si/W(500)/Ta(80)/ Cu(200)	Vacuum	30/723	
Si/W(50)/Cu	…	…/773	Reaction at 873
Si/Ta(180)/Cu(260)	Vacuum	30/873	$TaSi_2$ and Cu_3Si 30/923
Si/a-$Ta_{74}Si_{26}$(100)/ Cu(360)	Vacuum	30/873	30/923 by Cu induced crystallization of $Ta_{74}Si_{26}$ film
Si/a-$Ta_{36}Si_{14}N_{50}$(120)/ Cu(280)	Vacuum	30/1173	30/1223 $Ta_{36}Si_{14}N_{50}$ crystallizes
Si/a-$TiPN_2$(80)/Cu(250)	Vacuum	30/873	Fail structurally and electrically at 30/923
Si/$TiSi_2$(40)/a-$TiPN_2$(80)/ Cu(250)	Vacuum	30/973	Fail both structurally and electrically at 30/823

Sample configuration (nm)	Annealing ambient	Barrier effective at (min/K)	Phase formation (min/K)
Si/a-$W_{72}Si_{18}$(2000)/ Cu(105)	Vacuum	60/973	Crystallizes at 60/1073
Si/a-$Ni_{60}Nb_{40}$(500)/ Cu(100)	6.6×10^{-5} atm	60/873	
Si/$Ni_{57}Nb_{42}$/Cu	…	…	Cu diffuses in NiNb, replacing Nb at 60/923
Si/$W_{85}Si_{15}$/Cu	…	60/873	Barrier crystallizes at 973
Si/$Ni_{60}Mo_{40}$/Cu	…	…	60/773
Si/a-$Ir_{45}Ta_{55}$(30)/ Cu(50)/a-$Ir_{45}Ta_{55}$(30)	Vacuum	30/973	Cu diffuses in Si at 30/1023
Si/PtSi/Ta(100)/ Cu(200)	N_2:H_2 = 9:1	30/473	Reaction at 30/573
Si/Ta(100)/Cu(200)	N_2:H_2 = 9:1	30/573	Reaction at 30/673
Si/PtSi/Cr(100)/ Cu(200)	N_2:H_2 = 9:1	30/473	Reaction at 30/573
Si/PtSi/Ti(100)/Cu(200)	N_2:H_2 = 9:1	30/473	Reaction at 30/573
Si/PtSi/W(100)/Cu(200)	N_2:H_2 = 9:1	30/473	Reaction at 30/573
Si/PtSi/a-C(100)/ Cu(200)	N_2:H_2 = 9:1	30/473	Reaction at 30/573
Si/$TiSi_2$/Ta(20)/Cu(200)/Ta(30)	N_2:H_2 = 9:1	…	Reaction at 30/673
Si/$TiSi_2$/W(200)/Cu/ Ta(30)	N_2:H_2 = 9:1	…	Reaction at 30/573
Si/$TiSi_2$/Ti(25)/TiN(25)/Cu/ Ta(30)	N_2:H_2 = 9:1	30/673	Reaction at 30/500
Si/$TiSi_2$/Ti/TiN/W/Ta/ Cu/Ta	N_2:H_2 = 9:1	30/873	Reaction at 30/973
Si/$CoSi_2$/TiN_x(50)/Cu	Vacuum	30/873	
Si/$CrSi_2$/TiN_x(50)/Cu	Vacuum	30/873	
Si/$TiSi_2$/TiN_x(50)/ Cu(50)	Vacuum	30/873	
Si/$Ta_{53}C_{47}$(25)/Cu(100)[a]	5%H_2/N_2	30/1023	$TaSi_2$ and copper silicides at 1073
Si/$Ta_{53}C_{47}$(5)/Cu(100)[a]	5%H_2/N_2	30/873	

Sample configuration (nm)	Annealing ambient	Barrier effective at (min/K)	Phase formation (min/K)
$Si/Ta_{40}C_{60}(25)/Cu(100)$[a]	$5\%H_2/N_2$	30/973	$TaSi_2$ and Cu_3Si at 30/923
$Si/Ta_{20}C_{80}(25)/Cu(100)$[a]	$5\%H_2/N_2$	30/773	Cu_3Si at 30/873
$Si/Ta_{54}N_{46}(25)/Cu(100)$[b]	$5\%H_2/N_2$	30/1073	
Si/Ta(12,5)/Zr(5)/Ta(12,5)/ Cu(100)[c]	Vacuum	30/1048	Cu_3Si at 30/1073
$Si/Ta_{43}Si_4N_{53}(30)/Cu(100)$[d]	Ar-H_2 (10%)	60/1073	Cu_3Si and $TaSi_2$ at 60/1123

[a] Not included in the original table, from ref. [76].

[b] Not included in the original table, from ref. [77].

[c] Not included in the original table, from ref. [78].

[d] Not included in the original table, from ref. [79].

There is also a possibility to use intermetallic compounds, which are in equilibrium with both the silicide used as transistor contact and copper. For example, titanium forms several silicides and intermetallic compounds with copper. There could exist compounds, which are in thermodynamic equilibrium with both a titanium silicide and copper. In order to investigate if such an equilibrium exists, one needs to calculate the ternary phase diagram or at least the copper rich part of it.

In modern semiconductor manufacturing, the temperatures after the contact metal deposition do not rise above 973 K. Thus, this could be set as an upper limit for the stability of metallization system and the metallization scheme should be stable for 30-60 min at this temperature [80].

In summary, the possible diffusion barrier structures can be listed also from the materials point of view (see also Ch.2.1):

1. Structures which are based on the elements *e.g.* Ta, Ti, W
2. Solid solutions *e.g.* Ti-W solid solution

3. Intermetallic compounds (*i.e.* $TiCu_x$)

4. Chemically stable compounds *e.g*. silicides, nitrides, carbides (TaC, Ta_2N *etc*.)

5. Metastable structures *e.g*. amorphous ternary films (TaSiN *etc*.).

In this thesis Ta and Ta-based barrier layers were chosen to be studied. Tantalum has many good properties from the diffusion barrier point of view. It has a high melting point (3293 K) and therefore expected to have high activation energy for both lattice and grain boundary diffusion. It does not form intermetallic compounds with copper and thus provides a stable interface between copper and tantalum. The reaction between silicon and tantalum is also known to require quite high temperatures (923 K) [61], in that way providing a reasonably stable Si/Ta interface. In addition tantalum forms a stable oxide (Ta_2O_5), which provides a protective layer against copper corrosion and improves adhesion to SiO_2. It has been experimentally verified that tantalum protects the underlying copper from oxidation until the tantalum layer has been completely transformed into Ta_2O_5 [81]. The binary TaC and Ta-nitride compounds rely on their excellent thermal stability as well. TaC and Ta_2N barrier layers, which were also studied in this thesis, are interstitial compounds, which are generally thermally very stable (both have melting points over 3273 K.). They are also chemically quite inert with respect to many metals and Si. The onset of reactions generally requires high temperatures. Thus, the stability of the Si/barrier interface can be expected to increase in comparison to Ta-barriers. Ta [78,82-90] and TaC [76,91] as well as Ta-nitrides [77,92-103] have been frequently suggested to be used as diffusion barriers. Despite the relatively large amount of publications on Ta-based diffusion barriers, reaction mechanisms, phase formation sequence etc. have not been unambiguously solved. Hence, there was a need for more detailed studies.

3. Summary of the thesis

The object of the present work was to obtain a better understanding of the failure mechanisms, resulting microstructures and stabilities of the Ta-based barrier layers. The combined thermodynamic-kinetic approach, which has not been previously used in the

investigation of thin film diffusion barriers, was utilized for explaining the experimentally observed reaction sequences. It has been shown that this approach provides a better understanding about the reactions taking place during the annealings in the metallization structures.

The results show that Ta-based barriers offer a very feasible solution to the diffusion barrier problem. The failure mechanisms of the different barrier layers (*e.g.* Ta, TaC and Ta_2N) have many similarities. Especially, TaC and Ta_2N behave almost identically, as observed in Publication IV. With the help of thermodynamic evaluation of the corresponding ternary phase diagrams, we demonstrated that the reason behind this similarity was the almost identical phase relationships found in both metallization systems. In the case of elemental Ta diffusion barriers, we were also able to demonstrate that the failure mechanism was thickness dependent. Using this information, it was possible to explain many contradictions with respect to first phase formation during the annealings in the Si/Ta/Cu metallization system, as reported in the literature. Finally, the crucial effect of oxygen on the reactions in all the metallization schemes with different Ta-based diffusion barriers was shown and the thermodynamic basis for understanding the origins of this behavior was provided.

This thesis consists of five publications. The main results of each publication are summarized as follows:

In Publication I entitled, "Chemical Stability of Tantalum Diffusion Barrier Between Cu and Si", the first attempt was established to use the combined thermodynamic-kinetic approach for the diffusion barrier problem. The phases formed during the annealing were identified with XRD and SEM investigations. The ternary Ta-Si-Cu phase diagram was also evaluated in this study. Although the phase formation sequence was wrongly interpreted due to the lack of detailed experimental information, the use of combined thermodynamic-kinetic approach proved to be very helpful.

Publication II entitled, "Failure Mechanism of Ta Diffusion Barrier Between Cu and Si", is concentrated on the detailed reaction mechanism and sequence behind the failure in the Si/Ta/Cu metallization system. With careful TEM analyses combined with XRD results, we were able to show the thickness dependence of the phase formation sequence during the annealings. We demonstrated that, if the Ta barrier layer was about 100 nm thick the first phase to form was $TaSi_2$, which was followed by the formation of Cu_3Si. However, if the Ta thickness was in the order of 10-50 nm Cu_3Si formation took place first. With the help of this observation, we were able to explain many results found in the literature, which seemed to be in contradiction. Moreover, in this publication, we observed that oxygen plays an essential role in the reactions.

In publication III entitled, "Effect of Oxygen on the Reaction in the Si/Ta/Cu Metallization System", we explain - on a thermodynamic basis - the effect of oxygen on the reactions, which was first discovered in Publication II. We show that the formation of the metastable TaO_x took place at the Cu/Ta interface during the sputter-deposition, thus providing an additional barrier for Cu diffusion. By employing the assessed binary phase stability information we were also able to explain the following oxide dissolution. The presence of Ta-O type layer at the interface was experimentally verified with secondary ion mass spectrometry (SIMS) measurements.

Publication IV is entitled, "Tantalum Carbide and Nitride Diffusion Barriers for Cu Metallisation". In this publication, we observed that the behavior of the TaC and Ta_2N barrier layers was almost identical. We were able to reveal the reason behind these similarities. With the help of the Si-Ta-C, Si-Ta-N, Ta-C-Cu and Ta-N-Cu ternary phase diagrams, we could demonstrate that the phase relationships in the different systems were almost the same. This was the underlying reason for the nearly identical behavior. In this publication the strong effect of oxygen on reactions in both metallization systems was also observed.

In publication V entitled, "Stability of TaC Diffusion Barrier Between Si and Cu", results from the experimental and the thermodynamic-kinetic studies concerning the

failure mechanism of the TaC diffusion barrier were presented. The aim was to obtain better understanding about the reactions taking place in the system. We were able to show that despite the good "overall" stability of the TaC barrier layer the effect of oxygen on the reactions was again of utmost importance. With the help of high resolution electron microscopy we could detect an amorphous $Ta[O,C]_x$ layer at the TaC/Cu interface at 873 K, when the complete failure occurred only at 1023 K. The reaction sequence at the Si/TaC interface leading to the observed reaction structure was explained with the help of ternary phase diagrams and calculated activity diagrams. The publication also provides the thermodynamic basis to understand the formation of amorphous layer at the TaC/Cu interface. The formation of metastable $Ta[O,C]_x$ layer at the TaC/Cu interface at the expense of TaC layer resulted from the entrapped oxygen in the TaC films incorporated there during the sputter-deposition. We show that according to the metastable ternary Ta-C-O phase diagram evaluated at 873 K, in the presence of oxygen the excess carbon in the TaC films (as detected with RBS) can lead to the formation of Ta-oxide and graphite, thus providing the thermodynamic explanation for the observed amorphous phase formation.

References:

1. S.P. Murarka, "Advanced Materials for Future Interconnections of the Future Need and Strategy", Microelectronic Engineering, **37/38** (1997), 29.
2. J.T. Yue, "Reliability", in *ULSI Technology*, (Eds. C.Y. Chang and S.M. Sze) McGraw-Hill, USA, (1996), pp. 656-704.
3. J. Torres., "Advanced Copper Interconnections for Silicon CMOS Technologies", Appl. Surf. Sci., **91**, (1995), 112.
4. A. Broniatowski, " Multicarrier Trapping by Copper Microprecipitates in Silicon", Phys. Rev. Lett., **62**, (1989), 3074.
5. A.A. Istratov and E.R. Weber, "Electrical Properties and Recombination Activity of Copper, Nickel and Cobolt in Silicon", Appl. Phys. A, **66**, (1998), 123.
6. C-A. Chang, "Formation of Copper Silicides from Cu(100)/Si(100) and Cu(111)/Si(111) Structures", J. Appl. Phys., **67**, (1990), 566.
7. J. Li and J.W.Mayer," Refractory Metal Nitride Encapsulating for Copper Wiring", MRS Bulletin, **18**, (1993), 52.
8. F. Faupel, "Diffusion in Non-Crystalline Metallic and Organic Media", Phys. Stat. Sol. (a), **134**, (1992), 9.
9. S. Lakshminarayanan, J. Steigerwald, D.T.Price, M. Bourgwois, T.P.Chow, R.J. Gutman and S.P. Murarka, "Contact and Via Structures with Copper Interconnects Fabricated Using Dual Damascene Technology", IEEE Electr. Dev. Lett., **15**, (1994), 307.
10. S.P. Murarka,"Multilevel Interconnections for ULSI and GSI Era", Mater. Sci. Engineer.Rep., **R19**, (1997), 87.
11. B.J. Howard and Ch. Steinbruchel, "Reactive Ion Etching of Copper in $SiCl_4$ Based Plasmas", Appl. Phys. Lett., **59**, (1991)., 914.
12. M. Fayolle and F. Romagna, "Copper CMP Evaluation: Planarization Issues", Microelectronic Engineering, **37/38**, (1997), 135.
13. R. DeJule, "CMP Grows in Sophistication", Semiconductor International, **21**, (1998), 56.

14. M. Fury, "CMP Processing with Low-k Dielectrics", Sol. Stat. Tech., **42**, (1999), 87.
15. C.R.M. Grovenor, *Microelectronic Materials*, IOP Publishing (1989).
16. M-A. Nicolet, "Diffusion Barriers in Thin Films", Thin Solid Films, **52**, (1978), 415.
17. H.P. Kattelus and M-A. Nicolet, "Diffusion Barriers in Semiconductor Contact Metallization", in *Diffusion Phenomena in Thin Films and Microelectronic Materials*, (Eds. D. Gupta and P.S. Ho), Noyes Publication, Park Ridge, New Jersey, (1988).
18. R. Baluffi and J.M. Blakely, "Special Aspects of Diffusion in Thin Films", Thin Solid Films, **25**, (1975), 363.
19. L. Darken and R. Gurry, *Physical Chemistry of Metals*, McGraw-Hill, (1953).
20. E.A. Guggenheim, *Thermodynamics*, Elsevier Science, The Neatherlands, (1967).
21. G.N. Lewis and M. Randall, *Thermodynamics*, revised by K. Pitzer and L. Brewer, McGraw-Hill, (1961).
22. M. Hillert, "The Uses of Gibbs Free Energy-Composition Diagrams", in *Lectures on the Theory of Phase Transformations*, (Ed. H.I. Aaronson, AIME, (1975)).
23. N.A. Gokcen, *Thermodynamics*, Techscience Incorporated, (1975).
24. N. Saunders and A.P. Miodownik, *CALPHAD, Calculation of Phase Diagrams*, Pergammon Materials Series, Elsevier Science, (1998).
25. G.W. Castellan, *Physical Chemistry*, Addison Wesley, (1971).
26. O. Kubaschewski, O. Knacke and K. Hesselmann, *Thermochemical properties of inorganic substances*, Springer-Verlag, (1991).
27. A.D. Pelton and H. Schmalzried, "On the Geometrical Representation of Phase Equilibria", Metall. Trans., **4**, (1973), 1395.
28. L. Kaufman and H. Bernstein, *Computer Calculation of Phase Diagrams*, Academic Press, New York, (1970).
29. I. Ansara, " Thermodynamic Modelling of Solution Phases and Phase Diagram Calculations", Pure Appl. Chem., **62**, (1990), 71.
30. M. Hillert, *Phase Equilibria, Phase Diagrams and Phase Transformations : Their Thermodynamic Basis*, Cambridge Univ. Press, (1998).

31. P. Shewmon, *Diffusion in Solids*, TMS, USA, (1989).
32. J.S. Kirkaldy and D.J. Young, *Diffusion in the Condensed State*, The Institute of Metals, UK, (1987).
33. J. Philibert, *Atom Movements, Diffusion and Mass Transport in Solids*, Les Editions de Physique, France, (1991).
34. F.J.J. van Loo, "Multiphase Diffusion in Binary and Ternary Solid-State Systems", Prog. Solid St. Chem., **20**, (1990). 47.
35. J. Gulpen, "Reactive Phase Formation in the Ni-Si System", Doctoral Thesis, Technical University of Eindhoven, The Netherlands, (1995).
36. M.A. Dayananda, "Diffusion in Multicomponent Alloys: Challenges and Problems", Defect and Diffusion Forum, **83**, (1992), 73.
37. S. Tsuji, "Multiphase Binary Diffusion in Infinite and Semi-Infinite Media: Part I. On the Determination of Interdiffusion Coefficients", Metall. Mater. Trans. A, **25A**, (1994), 741.
38. S. Tsuji, "Multiphase Binary Diffusion in Infinite and Semi-Infinite Media: Part II. On the Numerical Calculation of the Rate Constants for Formation of Product Phases", Metall. Mater. Trans. A, **25A**, (1994), 753.
39. M.A. Dayananda and Y.H. Sohn, "Average Effective Interdiffusion Coefficients and Their Applications for Isothermal Multicomponent Diffusion Couples", Scr. Mater., **35**, (1996), 683.
40. M. Brown and M.F. Ashby, "Correlations for Diffusion Constants", Acta Metall., **28**, (1980), 1085.
41. P. Gas, "Diffusion in Silicides: Basic Approach and Practical Applications", in *Silicides: Fundamentals and Applications*, (Eds. L. Miglio and F. d'Heurle), World Scientific, (2001), pp. 34-51.
42. P. Gas and F.M. d'Heurle, "Formation of Silicide Thin Films by Solid State Reaction", App. Surf. Sci.,**73**, (1993), 153.
43. V. Dybkov, "Reaction Diffusion in Heterogeneous Binary Systems: Part 2 Growth of the chemical compound layers at the interface between two elementary substances: two compound layers", J. Mater. Sci., **21**, (1986), 3085.

44. V. Dybkov, "Solid State Growth Kinetics of the Same Chemical Compound Layer in Various Diffusion Couples", J. Phys. Chem. Solids, **47**, (1986), 735.
45. V. Dybkov, ""Reaction Diffusion in Heterogeneous Binary Systems: Part 3 Multiphase growth of the chemical compound layers at the interface between two mutually insoluble substances", J. Mater. Sci., **22**, (1987), 4233.
46. J. Philibert, "Reactive Interdiffusion", Materials Science Forum, **155-156**, (1994), 15.
47. F.M. d' Heurle, "The Kinetics of Reactive Phase Formation: Silicides", in *Silicides: Fundamentals and Applications*, (Eds. L. Miglio and F. d'Heurle), World Scientific, (2001), pp. 169-186.
48. U. Gösele and K.N. Tu, "Growth Kinetics of Planar Diffusion Couples:"Thin-Film Case" versus Bulk Cases", J. Appl. Phys., **53**, (1982), 3252.
49. R. Bormann, "Kinetics of Interface Reactions in Polycrystalline Thin Films", Mat. Res. Soc. Symp. Proc., **343**, (1994), 169.
50. A. Kodentsov, J. Gulpen, F.J.J. van Loo, C. Cserhati, and J.K. Kivilahti, "High-Temperature Nitridation of Ni-Cr Alloys", Metall.Trans.A, **27A**, (1996), 59.
51. T. Chou and Y. Chou, "Up-Hill Diffusion of Hafnium in Ni_3Al Intermetallic Alloys", Mater. Lett., **4**, (1986), 423.
52. J. Ågren, "A Note on the Theoretical Treatment of Up-Hill Diffusion in Compound Welds", Metall. Trans. A, **14A**, (1983), 2167.
53. T. Tsakalakos and M. Dugan," Nonlinear Diffusion in Spinodal Decomposition: a Numerical Solution", J. Mater. Sci., **20**, (1985), 1301.
54. J.S. Kirkaldy, "Diffusion in Multicomponent Metallic Systems", Can. J. Phys., **36**, (1958), 899.
55. J.S. Kirkaldy and L.C. Brown, "Diffusion Behaviour in Ternary, Multiphase Systems", Can. Met. Q., **2**, (1963), 89.
56. D. Coates and J.S.Kirkaldy,"Phase Interface Stability in Isothermal Ternary Systems" Proc. Second Internat. Conf. on Crystal Growth, North-Holland Publishing, Amsterdam, (1968), pp. 549-554.
57. K. Bhanumurthy and R. Schmid-Fetzer, "Solid State Phase Equilibria and Reactive Diffusion in the Cr-Si-C System", Z. Metallkd., **87**, (1996), 61.

58. T. Laurila, K. Zeng, J.K. Kivilahti, J. Molarius and I. Suni, "TaC as a Diffusion Barrier Between Si and Cu", J. Appl. Phys., (submitted).

59. J. Philibert, "Reactive Diffusion in Thin Films", Appl. Surf. Sci., **53**, (1991), 74.

60. I. Kaur and W. Gust, *Fundamentals of Grain and Interphase Boundary Diffusion*, Ziegler Press, (1989).

61. G. Ottaviani, "Metallurgical Aspects of the Formation of Silicides", Thin Solid Films, **140**, (1986), 3.

62. A. Christou and H.M. Day, "Silicide Formation and Interdiffusion Effects in Si-Ta, SiO_2-Ta and Si-PtSi-Ta Thin Film Structures" J. Electr. Mater., **5**, 1976, 1.

63. J.G.M.Becht, "The Influence of Phosphorous on the Solid State Reaction Between Copper and Silicon or Germanium", Doctoral Thesis, Tech. University of Eindhoven Netherlands, (1987).

64. E. Hondros and M. Seah, "Segregation to Interfaces", Int. Met. Rev, **22**, (1977), 262.

65. E. Hondros and M. Seah, "The Theory of Grain Boundary Segragation in Terms of Surface Adsorption Analogues", Metall. Trans. A, **8A**, (1977), 1363.

66. M. Guttmann, "Grain Boundary Segregation, Two Dimensional Compound Formation, and Precipitation", Metall. Trans. A, **8A**, (1977), 1383.

67. P.Pokela., "Amorphous Diffusion Barriers for Electronic Device Applications", Doctoral Thesis., Helsinki University of Technology, (1991).

68. E. Kolawa, P.Pokela, J. Reid, J. Chen, R. Ruiz and M-A. Nicolet, "Sputtered Ta-Si-N Diffusion Barriers in Cu Metallizations for Si", IEEE Electr. Dev. Lett., **12**, (1991), 321.

69. E. Kolawa, J.M. Molarius, C.W. Nieh and M-A. Nicolet, "Amorphous Ta-Si-N Thin-Film Alloys as Diffusion Barrier in Al/Si Metallizations", J. Vac. Sci. Tech., **A8,** (1990), 3006.

70. J.M. Molarius, E. Kolawa, K. Morishita, M-A. Nicolet, J.L. Tandon, J.A. Leavitt and L.C. McIntyre Jr., "Tantalum-Based Encapsulants for Thermal Annealing of GaAs", J. Electrochem. Soc., **138**, (1991), 834.

71. M. Kijek, M. Ahmadzadeh, B. Cantor and R.W. Cahn, "Diffusion in Amorphous Alloys", Scr. Metall., **14**, (1980), 1337.

72. H.Holleck, M. Lahres, and P. Woll," Multilayer Coatings-Influence of Fabrication Parameters on Constitution and Properties", Surf. and Coat. Tech., **41**, (1990), 179.

73. O. Knotek, A.Barimani, and F. Löffler, "On the Formation of Amorphous and Metastable PVD-Coatings", in *Thin film structures and phase stability : symposium* held April 16-17, 1990, San Francisco, California, U.S.A., ed. Clemens, B. M.

74. M.A. Nicolet, in: *Diffusion in Amorphous Materials,* eds. H. Jain and D. Gupta, (TMS Warrendale, 1994), pp. 225-234.

75. S-Q. Wang, S. Suthar, K. Hoeflich, and B.J. Burrow,"Diffusion Barrier Properties of TiW Between Si and Cu", J. Appl. Phys., **73**, (1993), 2301.

76. J. Imahori, T. Oku, and M. Murakami,"Diffusion Barrier Properties of TaC Between Si and Cu", Thin Solid Films, **301**, 1996, 142.

77. T. Oku, E. Kawakami, M. Uekebo, K. Takahiro, S. Yamaguchi, and M. Murakami,"Diffusion Barrier Property of TaN Between Si and Cu", Appl. Surf. Sci., **99**, (1996), 265 .

78. J. Kwak, H-K. Baik, J-H. Kim and S-M. Lee, "Improvement of Ta Diffusion Barrier Performance in Cu Metallization by Insertion of a Thin Zr Layer into Ta Film", Appl. Phys. Lett., **72**, (1998), 2832.

79. Y-J. Lee, B-S. Suh, S-K. Rha, and C-O. Park, "Structural and Chemical Stability of Ta-Si-N Thin Film Between Si and Cu", Thin Solid Films, **320**, (1998), 141.

80. S.P. Murarka, *Metallization: Theory and practice for VLSI and ULSI*, Butterworth-Heinemann, (1993).

81. T. Ichikawa, M. Takeyama, and A. Noya," Oxidation Behavior of Ta Thin Films as a Passivation Layer Deposited on Cu", Jpn. J. Appl. Phys., **35**, (1996), 1844.

82. K. Holloway and P. Fryer, " Tantalum as a Diffusion Barrier Between Copper and Silicon", Appl. Phys. Lett., **57**, (1990), 1736.

83. K. Holloway, P. Fryer, C. Cabral, J. Harper, P. Bailey, and Kelleher, K., "Tantalum as a Diffusion Barrier Between Copper and Silicon: Failure Mechanism and Effect of Nitrogen Additions ", J. Appl. Phys., **71**, (1992), 5433.

84. S. Jang, S-M. Lee, and H-K-. Baik, " Tantalum and Niobium as a Diffusion Barrier Between Copper and Silicon", J. Mater. Sci: Mater. in Electr., **7**, (1996), 271.

85. B. Kang, S-M. Lee, J. Kwak, D. Soon, and H-K. Baik, " The Effectiveness of Ta Prepared by Ion-Assisted Deposition as a Diffusion Barrier Between Copper and Silicon", J. Electrochem. Soc., **144**, (1997), 1807.

86. L. Lane, T. Nason, G-R. Yang, T-M. Lu and H. Bakhru,"Secondary Ion Mass Spectrometry Study of the Thermal Stability of Cu/Refractory Metal/Si Structures", J. Appl. Phys., **69**, (1991), 6719.

87. K-M. Yin, L. Chang, F-R. Chen, J-J. Kai, C-C. Chiang, P. Ding, B. Chin, H. Zhang and F. Chen, "The Effect of Oxygen in the Annealing Ambient on Interfacial Reactions of Cu/Ta/Si Multilayers", Thin Solid Films, **388**, (2001), 15.

88. K-M. Yin, L. Chang, F-R. Chen, J-J. Kai, C-C. Chiang, G. Chuang, P. Ding, B. Chin, H. Zhang and F. Chen, "Oxidation of Ta Diffusion Barrier Layer for Cu Metallization in Thermal Annealing", Thin Solid Films, **388**, (2001), 27.

89. D.Yoon, , H. Baik, and S-M., Lee, "Tantalum-Microcrystalline CeO_2 Diffusion Barrier for Copper Metallization", J. Appl. Phys., **83**, (1998), 1333.

90. D. Yoon, H. Baik, and S-M. Lee, "Effect on Thermal Stability of a Cu/Ta/Si Heterostructure of the Incorporation of Cerium Oxide into the Ta Barrier", J. Appl. Phys., **83**, (1998), 8074.

91. H. Tsai, S. Sun, and S. Wang,"Characterization of Sputtered Tantalum Carbide Barrier Layer for Copper Metallization", J. Electrochem. Soc., **147**, (2000), 2766.

92. M. Tsai, S. Sun, H. Chiu, C. Tsai, and S. Chuang, " Metalorganic Chemical Vapor Deposition of Tantalum Nitride by Tertbutylimidotrist(diethylamido) tantalum for Advanced Metallization", Appl. Phys. Lett., **67**, (1995), 1128.

93. S. Sun, M. Tsai, C. Tsai, and H. Chiu, " Performance of MOCVD Tantalum Nitride Diffusion Barrier for Copper Metallization", 1995 Symposium on VLSI technology digest of technical papers, (1995), 29.

94. M. Tsai, S. Sun, C. Lee, H. Chiu, C. Tsai, S. Chuang, and S. Wu, " Metal-Organic Chemical Vapor Deposition of Tantalum Nitride Barrier Layers for ULSI Applications", Thin Solid Films, **270**, (1995), 531.

95. S. Nakao, M. Numata, and T, Ohmi, " Thin and Low-Resistivity Tantalum Nitride Diffusion Barrier and Giant-Grain Copper Interconnects for Advanced ULSI Metallization", Jpn. J. Appl. Phys, **38**, (1999), 2401.

96. C. Xiaomeng, H. Frisch, A. Kaloyeros, B. Arkles, and J. Sullivan, " Low Temperature Plasma-Assisted Chemical Vapor Deposition of Tantalum Nitride from Tantalum Pentabromide for Copper Metallization", J. Vac. Sci. Tech., **B17**, (1999), 182.

97. A. Kaloyeros, C. Xiaomeng, T. Stark, K. Kumar, C. Soon, G. Peterson, H. Frisch, B. Arkles, and J. Sullivan, " Tantalum Nitride Films Grown by Inorganic Low Temperature Thermal Chemical Vapor Deposition-Diffusion Barrier Properties in Copper Metallization", J. Electrochem. Soc., **146**, (1999), 170.

98. L. Sung, B. Ki, H. Seok, K. Hyun, and D. Sam, " Diffusion Barrier Properties of Metallorganic Chemical Vapor Deposited Tantalum Nitride Films Against Cu Metallization", J. Electrochem. Soc., **146**, (1999), 3724.

99. G. Chen, S. Chen, L-C. Yang, and P. Lee, " Evaluation of Single- and Multilayered Amorphous Tantalum Nitride Thin Films as Diffusion Barriers in Copper Metallization", J. Vac. Sci. Tech., **A18**, (2000), 720.

100. G. Chen, S. Huang, S. Chen, T. Yang, P. Lee, J. Jou, and T. Lin, " An Optimal Quasisuperlattice Design to Further Improve Thermal Stability of Tantalum Nitride Diffusion Barriers", Appl. Phys. Lett., **76**, (2000), 2895.

101. G. Chen and S. Chen, "Diffusion Barrier Properties of Single- and Multilayered Quasi-Amorphous Tantalum Nitride Thin Films Against Copper Penetration", J. Appl. Phys., **87**, (2000), 8473.

102. K. Yap, H. Gong, J. Dai, T. Osipowicz, L. Chan, and S. Lahiri, "Integrity of Copper-Tantalum Nitride Metallization Under Different Ambient Conditions", J. Electrochem. Soc., **147**, (2000), 2312.

103. M. Yanjun, D. Tweet, L. Charneski, and D. Evans, "Density oscillation in Sputtered Tantalum Nitride Barrier Metal Thin Films", Advanced Metallization Conference in 1998 (AMC 1998). Proceedings of the Conference. Mater. Res. Soc, Warrendale, PA, USA, (1999), 357.